Ore Geology Reviews 155 (2023) 105369

Contents lists available at ScienceDirect

Ore Geology Reviews

journal homepage: www.elsevier.com/locate/oregeorev

The Dugald River-type, shear zone hosted, Zn-Pb-Ag mineralisation, Mount Isa Inlier, Australia

Pieter K. Creus [a,*], Ioan V. Sanislav [a], Paul H.G.M. Dirks [a], Corey M. Jago [b], Brett K. Davis [c]

[a] Economic Geology Research Centre (EGRU) and Department of Earth and Environmental Sciences, James Cook University, Townsville, Queensland 4811, Australia
[b] MMG Rosebery, PO Box 21, Rosebery, Tasmania 7470, Australia
[c] Olinda Gold Pty Ltd, 131 Vines Avenue, The Vines, Western Australia 6069, Australia

ARTICLE INFO

Keywords:
Zn-Pb-Ag Mineralisation
Mount Isa Inlier
Shear Zone Hosted Mineralisation
Durchbewegung Texture
Epigenetic Breccia Ore

ABSTRACT

The Dugald River Zn-Pb-Ag mine is situated in the Mount Isa Inlier, a globally significant base metal province. Zn-Pb deposits in the Mount Isa Inlier are stratabound with four main genetic models, including SEDEX-style, remobilised SEDEX, epigenetic and Broken Hill-type mineralisation applied to interpret their formation. We propose that the Zn-Pb-Ag mineralisation at Dugald River represents a unique, shear zone hosted deposit type that formed through a series of successive deformation events during the Paleoproterozoic Isan Orogeny that concentrated the mineralisation within the Dugald River Shear Zone during two main mineralising phases. The first phase of mineralisation occurred during regional D_2 shortening, which is associated with the formation of large-scale F_2 folds and a regionally penetrative S_2 fabric. During this phase, progressive tightening of upright F_2 folds resulted in several sets of secondary space accommodating quartz-carbonate veins that were progressively rotated into parallelism with the pervasive, steep, W-dipping S_2 cleavage. The quartz-carbonate veins were coevally replaced by sulphides, which migrated to extensional sites (boudin necks and fold hinges) in tight folds. Thereby creating a sulphide-rich horizon within a developing high strain zone, which during D_4 developed into the Dugald River Shear Zone. The second phase of mineralisation occurred during the regional D_4 transpressional deformation event and resulted in significant metal enrichment and the current geometry of the ore bodies. The significant enrichment of the mineralisation during D_4 resulted from further fold tightening within the high strain zone, which resulted in the attenuation and dismembering of folds and produced a transposed fabric (S_4). The sulphide veins were transposed into parallelism with S_4 forming sulphide-rich planar ore textures. Strain partitioning at the contact between the ductile deforming sulphide horizon and the brittle deforming slates resulted in the development of an anastomosing shear zone, known as the Dugald River Shear Zone. A right-handed releasing bend in the shear zone produced a dilational jog and a thick, high-grade ore body. The mobilisation of sulphides within the dilational jog involved fragmentation of sulphides and wall rock, brecciation, rotation and rolling of fragments, and the formation of durchbewegung texture.

1. Introduction

The Mount Isa Inlier, located in NW Queensland, is a globally significant base metal province (Fig. 1). World-class Zn-Pb deposits (Fig. 1c) include the Mt Isa deposit (e.g., Smith et al., 1978; Gulson et al., 1983; McGoldrick and Keays, 1990; Perkins, 1997; Davis, 2004; Cave et al., 2020), the Cannington deposit (e.g., Bodon, 1998; 2002; Roache et al., 2004; Walters and Bailey, 1998), the George Fisher and Hilton deposits (Valenta, 1994a; b; Perkins and Bell, 1998; Chapman, 2004; Murphy, 2004; Cave et al., 2020) and the Dugald River deposit (Newbery et al., 1993; Xu, 1996; 1997; 1998a; b; Creus, 2022). The Zn-Pb mineralisation style extends further north to the McArthur Basin to include Century, McArthur River (HYC) and Teena deposits (Broadbent et al., 1998; Feltrin et al., 2009; O'Rourke et al., 2017; Sheldon et al., 2021). Together these deposits form the largest Zn-Pb province in the world (Huston et al., 2006).

Although the deposits display similarities in primary metal content (Zn-Pb), ore mineralogy (namely sphalerite and galena) and host rock type (mainly siliciclastic metasediments), the structural and metamorphic settings are variable. As a result, genetic models for the deposits vary as well. For example, in the Mount Isa town region in the west, the metamorphic grade of host lithologies varies from sub-greenschist facies

* Corresponding author.
E-mail address: pieter.creus@my.jcu.edu.au (P.K. Creus).

https://doi.org/10.1016/j.oregeorev.2023.105369
Received 22 October 2022; Received in revised form 21 February 2023; Accepted 23 February 2023
Available online 28 February 2023

in the George Fisher and Hilton deposits (see Rieger et al., 2021) to upper amphibolite facies in the Cannington deposit (see Chapman and Williams, 1998), thus the metamorphic grade increases from northwest to southeast (Fig. 2). Four genetic models for the Zn-Pb deposits have been proposed: 1) syngenetic-SEDEX style mineralisation (e.g., Smith et al., 1978; Large et al., 2005); 2) remobilised SEDEX style mineralisation (e.g., Finlow-Bates and Stumpfl, 1979; McGoldrick and Keays, 1990); 3) epigenetic mineralisation (e.g., Xu, 1996; Davis, 2004) and 4) Broken Hill type mineralisation (Walters and Bailey, 1998). It should be noted that all Zn-Pb deposits of the Mount Isa Inlier are stratabound, although the mineralisation can be discordant.

A syngenetic origin for some of the deposits (e.g., Mt Isa, George Fisher and Hilton) is supported by the preservation of *syn*-sedimentary textures. Fine-grained sphalerite and galena occur in thin laminae and bands parallel with the sedimentary layering as well as the preservation of textures suggesting intergrowth of sphalerite and galena with framboidal pyrite (e.g., Cave et al., 2020; Rieger et al., 2021). Although late metasomatic and metamorphic overprints affected these deposits, early *syn*-sedimentary textures are locally preserved. Conversely, the Cannington deposit underwent high-grade metamorphism and intense metasomatism, making the identification of *syn*-sedimentary textures nearly impossible (e.g., Chapman and Williams, 1998; Walters and Bailey, 1998) and thus being in general classified as Broken Hill-type mineralisation (Walters and Bailey, 1998).

In this publication, we discuss the structural controls that lead to the formation of the Dugald River deposit. The deposit represents an ideal case study for metamorphosed Zn-Pb mineralisation as it can be considered an intermediate between weakly metamorphosed end members such as the George Fisher deposit (sub-greenschist facies) and intensely metamorphosed end members such as the Cannington deposit (upper amphibolite facies) and may represent a new type of Zn-Pb mineralisation in the Mount Isa Inlier. Although the mineralisation is

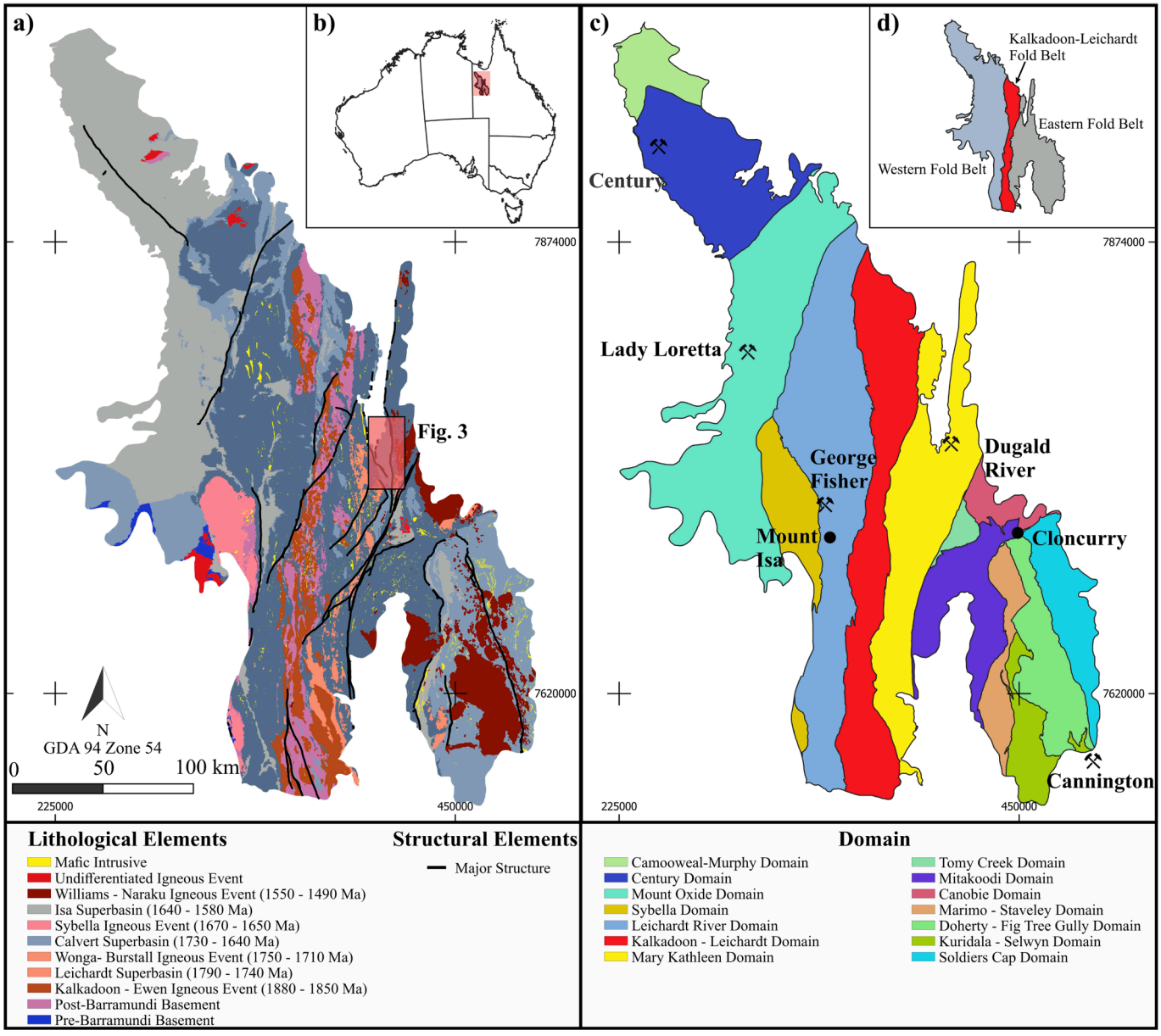

Fig. 1. A) volcano-sedimentary and igneous rocks of the mount isa inlier, nw queensland, Australia (b) clipped to the outcrop pattern of the Mount Isa Inlier. c) The Mount Isa Inlier is sub-divided into sixteen domains (fourteen shown here) and is usually presented in a simplified format and grouped into three fold belts, namely, the Western and Eastern Fold Belts, which are separated by the Kalkadoon-Leichardt Fold Belt (d). d) Historical grouping of the Mount Isa Inlier modified after Blake (1987).

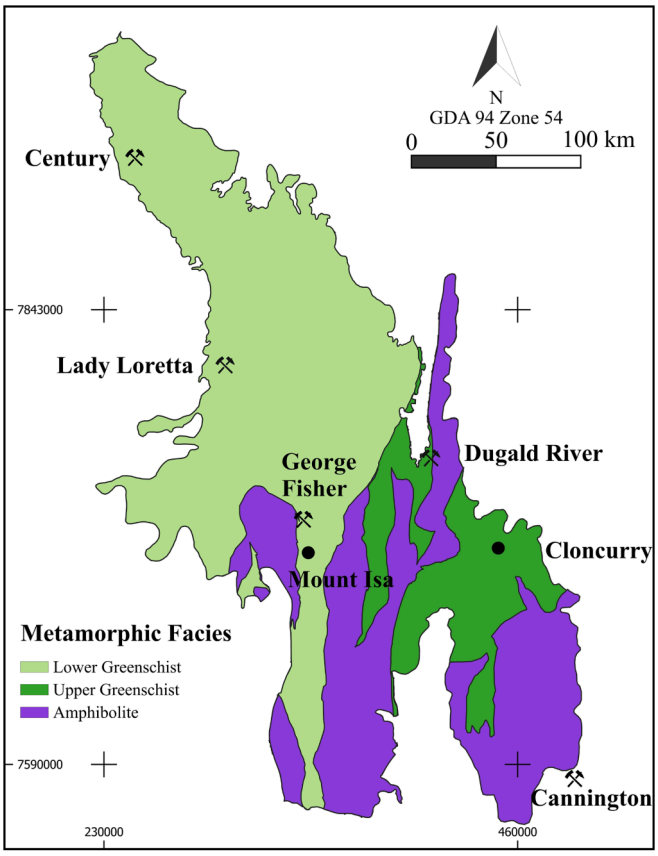

Fig 2. Metamorphic facies map of the Mount Isa Inlier modified from Foster and Rubenach (2006).

almost entirely hosted by a complex shear zone and the metamorphic grade reached amphibolite facies, the host rocks still preserve evidence of *syn*-sedimentary textures (*viz.* bedding and stratigraphy) and the structural evolution of the deposit can be reconstructed. The genetic model presented in this publication not only has implications for understanding the genesis of Zn-Pb mineralisation in metamorphic terranes but also for shear zone hosted Zn-Pb deposits in general.

2. Regional geology

The Dugald River Zn-Pb-Ag deposit is hosted by Late Paleoproterozoic rocks of the Mount Isa Inlier in NW Queensland, Australia. The Mount Isa Inlier consists of a succession of volcano-sedimentary and intrusive rocks formed during a series of successive basin and orogenic events between ~ 1900 – 1500 Ma (see Blake, 1987; Blake and Stewart, 1992; Foster and Austin, 2008; Gibson et al., 2016). Three superbasin events are recognised that are separated by regional unconformities (Fig. 1a; Betts et al., 2006; Gibson et al., 2016): 1) Leichardt Superbasin (1790–1740 Ma); 2) Calvert Superbasin (1730–1640 Ma); and 3) Isa Superbasin (1640–1580 Ma) that were deposited over the basement Leichardt Metamorphics, which have a formation age of between 1900 and 1850 Ma. The superbasins are vertically stacked and inferred to have formed during ≥1840 Ma continental rifting (Betts et al., 2006, 2008; Gibson et al., 2008; 2012; 2016) within which the depositional environment changed from fluviatile-lacustrine to open marine (Jackson et al., 2000; Southgate et al., 2000).

Three major orogenic events have affected the Mount Isa Inlier, the 1880 – 1850 Ma Barramundi Orogeny, the 1750–1710 Ma Wonga Orogeny and the 1650–1490 Ma Isan Orogeny (see Blake, 1987; Blake and Stewart, 1992; Foster and Austin, 2008; Abu Sharib and Sanislav, 2013; Spence et al., 2021; 2022). The Barramundi and Wonga Orogenies have only affected the basement and the older sedimentary units whereas the Isan Orogeny has affected the entire Mount Isa Inlier. Recent studies have indicated that parts of the Mount Isa Inlier were also affected by shortening events and associated magmatism between 1800 and 1770 Ma (Le et al., 2021a;b).

Four main periods of plutonism occurred in the Mount Isa Inlier. The plutons were emplaced along N-S trending linear belts with the first period between 1880 and 1850 Ma resulting in the emplacement of the Kalkadoon and Ewen Batholiths (Page, 1983; Page and Williams, 1988; Bierlein et al., 2011). The second period occurred between 1750 and 1710 Ma and coincided with the emplacement of the Wonga and Burstall plutons (Neumann et al., 2009; Spence et al., 2021; 2022). The third period occurred between 1670 and 1650 Ma and coincided with the emplacement of the Sybella Batholith (Page and Bell, 1986; Connors and Page, 1995) and the fourth period occurred between 1550 and 1490 Ma with the emplacement of the Williams-Naraku Batholiths (Page and Sun, 1998; Wyborn, 1998).

The Mount Isa Inlier is sub-divided into a series of sixteen N-S trending geological domains (Fig. 1c; Wellman and Dooley, 1992; Withnall and Hutton, 2013), based on differences in basin sequences, metamorphism, structural and intrusive history. The domains are generally bounded by crustal-scale faults and shears. The Dugald River deposit is situated within the Mary Kathleen Domain (yellow domain in Fig. 1c) and the geology is dominated by sedimentary sequences deposited during the evolution of the Leichhardt Superbasin (Gibson et al., 2016) and intruded by the Wonga and Burstall plutons between 1750 and 1710 Ma (Neumann et al., 2009; Spence et al., 2021). A series of younger sedimentary sequences unconformably overlie the Leichhardt Superbasin sedimentary rocks in the north of the domain and are collectively assigned to the Mount Albert Group (Derrick et al., 1977), which is part of the Calvert Superbasin (Gibson et al., 2016).

Five main deformation events have been recognised in the Mount Isa Inlier and allocated to the Isan Orogeny. The first event, D_1, occurred during N-S shortening and produced E-W trending regional folds and thrusts (Bell, 1983; Bell et al., 1992; Page and Bell, 1986; Blake and Stewart, 1992; Abu Sharib and Sanislav, 2013). The second event, D_2, occurred during E-W shortening and produced the main N-S trending folds, shear zones and thrusts that define the dominant structural grain of the Isan Orogeny (e.g., Bell et al., 1992; Giles et al., 2006; Abu Sharib and Bell, 2011; Abu Sharib and Sanislav, 2013). The third event, D_3, has been described as an orogenic collapse phase that crenulated D_2 fabrics and produced a sub-horizontal cleavage (e.g., Bell and Hickey, 1998; Davidson et al., 2002) that was later overprinted, during the fourth deformation event, D_4, by a new N-S trending cleavage. D_4 occurred during renewed E-W shortening, but with a pronounced transpressive character marked by a transition from ductile to brittle-ductile deformation (O'Dea et al., 1997; Bell and Hickey, 1998; Spampinato et al., 2015). The last major deformation event, D_5, occurred during ESE-WNW shortening and resulted in brittle reactivation of major structures and the development of an open to close crenulation cleavage in higher-grade rocks.

Multiple metamorphic events have been recognised as part of the Isan Orogeny (e.g., O'Dea et al., 1997; Rubenach et al., 2008; Sayab, 2009; Abu Sharib and Sanislav, 2013), that are characterised by low-pressure/high-temperature metamorphic assemblages (Connors et al., 1992; Foster and Rubenach, 2006). According to Abu Sharib and Sanislav (2013), high geothermal gradients (see Rubenach and Lewthwaite, 2002; Rubenach et al., 2008) associated with the emplacement of magmatic bodies provided enough heat for metamorphism during successive phases of the Isan Orogeny. They suggested that the M_1 metamorphic event during D_1 was low-pressure and high-temperature metamorphism accompanied by a period of NE-SW bulk shortening during the early stages of the Isan Orogeny.

Peak metamorphic conditions reached upper amphibolite facies in the Eastern Fold Belt (Loosveld and Schreurs, 1987; Foster and Rubenach, 2006), during the later stages of the E-W directed D_2 (O'Dea et al.,

1997), and possibly early into the D_3 (Blake and Stewart, 1992; Rubenach and Lewthwaite, 2002). Low-pressure and high-temperature clockwise P-T paths have been suggested for the M_2 metamorphic event during D_2 by numerous authors (e.g., Oliver et al., 1991; Reinhardt, 1992; Rubenach et al., 2008; Sayab, 2009; Abu Sharib and Sanislav, 2013). Foster and Rubenach (2006) provide a summary table of thermobarometric studies for select locations in the Mount Isa Inlier from which they suggest that the highest-grade zones are between 4 and 5 kbar and >650 °C. Furthermore, they found that in an E-W transect through the Mount Isa Inlier, metamorphic grade varies from lower greenschist to upper amphibolite facies and that the overall pattern of metamorphism is a series of N-S orientated amphibolite facies belts separated by greenschist facies belts (Fig. 2). Further north of Mount Isa, lower greenschist facies conditions are suggested (Gibson and Hitchman, 2005; Nortje et al., 2011) and substantiated by lower greenschist facies conditions for the Century deposit and unmetamorphosed for HYC in the MacArthur Basin to the northwest of the Mount Isa Inlier.

3. Dugald River deposit

The Dugald River deposit outcrops as a Zn-Pb-Fe-Mn gossan and was first discovered in 1881 and has been a drill target since 1948 (Connor et al., 1982; Xu, 1998b). Ownership of the exploration license for the deposit has changed several times and in 2009 MMG Ltd. undertook a feasibility study to commence mining. Underground development commenced in 2012 and production of Zn concentrate in 2017 with the 2020 resource stated at 66Mt with 11.7% Zn, 1.3% Pb and 26 g/t Ag

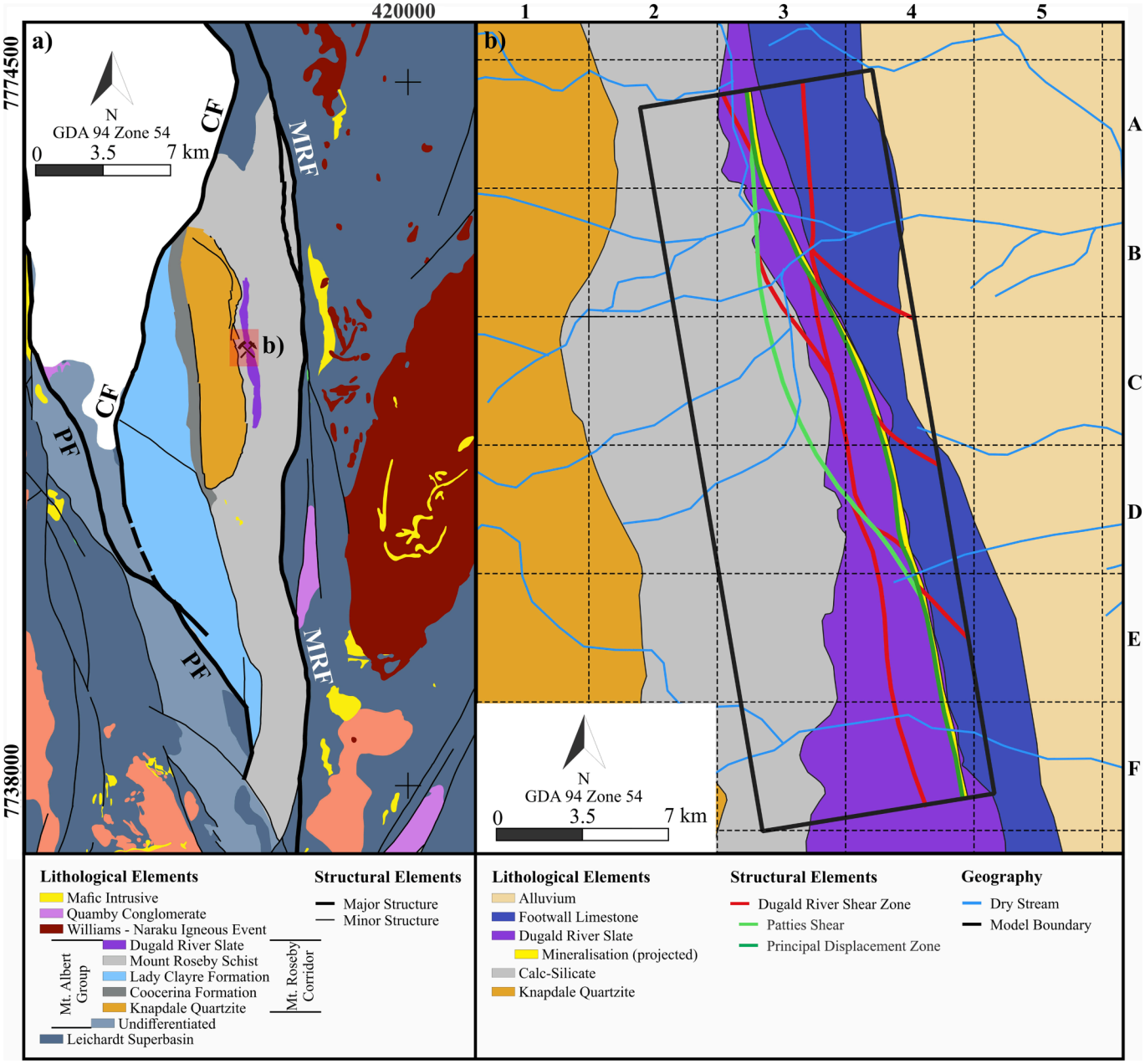

Fig. 3. A) the mount Roseby Corridor is an N-S trending high strain corridor of Mount Albert Group rocks, bounded to the east by the Mount Roseby Fault (MRF), the west by the Coolulah Fault (CF) and the southwest by the Pinnacle Fault (PF). b) Simplified geological map of the Dugald River deposit. The black outline is the 3D model boundary and envelopes the majority of the available data. The geological map has a local grid system used as a reference in this publication. Note, that the Patties Shear and principal displacement zone form part of the Dugald River Shear Zone.

(MMG, 2021). The deposit is wholly underground and accessed via two declines: one accessing the northern extent of the deposit ("North Mine") and the second, the southern extent of the deposit ("South Mine").

3.1. Lithostratigraphy

The Dugald River deposit is situated within the Mount Roseby Corridor (Fig. 3; Newbery et al., 1993). The Mount Roseby Corridor is a narrow, N-S trending zone of high strain rocks of the Mount Albert Group and bounded by major faults, the Mount Roseby Fault to the east, the Coolullah Fault to the west, and the Pinnacle Fault to the southwest.

The Mount Albert Group in the Mount Roseby Corridor has been subdivided into 4 main units: the Knapdale Quartzite, Lady Clayre Dolomite, Coocerina Formation, and the Mount Roseby Schist (Fig. 3a). The Mount Roseby Schist is a time equivalent of the Coocerina Formation and Lady Clayre Dolomite (Withnall and Hutton, 2013). The Knapdale Quartzite is interpreted to represent the oldest unit, flanked by the Mount Roseby Schist to the east and by the Coocerine Formation and Lady Clayre Dolomite to the west. The Dugald River deposit is hosted by the Dugald River Shale, which is a member of the Mount Roseby Schist Formation (ASUD, 2021). However, the Mount Roseby Schist has been metamorphosed to amphibolite facies and the Dugald River Shale has a prevalent slatey cleavage and will be referred to as the Dugald River Slate in this publication (also see Connor et al., 1982; Newbery et al., 1993; Xu, 1996).

The Mount Roseby Schist within the mine volume of interest (Fig. 3b) is subdivided into three main units (also see Connor et al., 1982; Newbery et al., 1993; Xu, 1996, ASUD, 2021). From oldest to youngest these are: 1) a calc-silicate unit; 2) the Dugald River Slate and 3) the Footwall Limestone. It should be noted that the Footwall Limestone is a mining term as it occurs along the footwall of the lode, but younging directions indicate it is stratigraphically younger than the Dugald River Slate that hosts the mineralisation (e.g., Newbery et al., 1993; Spelbrink and George, 2017). Minor lithological units found near the deposit include a mafic feldspar porphyry dyke and muscovite schists (Spelbrink and George, 2017).

The calc-silicate unit comprises two main varieties, biotite-garnet-scapolite schist and a carbonate-rich banded biotite-scapolite schist (Spelbrink and George, 2017). The scapolite and garnet form porphyroblasts observable in the hand sample. Under the petrographic microscope, they preserve a well-developed internal foliation defined by inclusion trails of unknown composition (Davis, 2017). The transition from calc-silicate to the Dugald River Slate is marked a high strain zone and consists of medium- to coarse-grained, banded biotite-epidote schist pods that have a strong schistosity. Within the high strain zone, lenses of a weakly deformed mafic feldspar porphyry dyke are common and the geometry of these lenses and the localisation of intense deformation along their margins suggest that the mafic dyke was boudinaged during shearing.

The Dugald River Slate is massive and fine-grained with a dark grey to black appearance depending on the graphite content. The slate has a spotted appearance in places due to scapolite porphyroblasts (Williams, 2017), which tend to have strain shadows (Fig. 4) with variable concentrations of carbonate, quartz, and sulphides. The scapolite porphyroblasts within the Dugald River Slate are aligned parallel to the main foliation. The muscovite schist forms discrete lenses within the Dugald River Slate that are inferred to be structurally controlled and display a strong anastomosing fabric (Spelbrink and George, 2017) and red garnet porphyroblasts are common.

The limestone occurs to the east of the lode. It is light to dark grey, with flattened sulphide streaks defining a trend similar to the main foliation (Newbery et al., 1993; Xu, 1996) and fine-grained, wispy discontinuous white carbonate veinlets (Spelbrink and George, 2017) defining an S_3 spaced cleavage. Bedding is preserved within the limestone and is defined by dark grey, massive dolomitic layers intercalated with mica, quartz and K-feldspar rich layers. Scapolite porphyroblasts are common and contain strain shadows which are aligned sub-parallel to the main fabric.

3.2. Deformational history

The Mount Roseby Schist at Dugald River has been subjected to up to five deformational events. Structures produced during the first deformation event, D_1, have largely been overprinted by E-W, co-planar shortening during D_2 and D_4. The first three deformational events are inferred to be ductile, followed by brittle-ductile deformation during D_4, and D_5 which represents a period of brittle reactivation of mainly D_4 structures. Recognising primary textures and features in the underground workings (including drill intersections) is difficult not only due to the dark colour of the rock but mainly due to the intense deformation which has obliterated earlier tectonic fabric, including those produced during D_1.

3.2.1. D_1 structures

The earliest deformation event, D_1, recognised at the Dugald River deposit is defined by a series of E-W trending folds (F_1) and associated axial planar cleavage (S_1) which resulted from N-S shortening (Xu, 1996). Broad F_1 folds are observed to the south of the deposit where they occur as metre-scale folds refolded during D_2 along N-S trending axes in Type 1 interference pattern and F_1 are exposed 10 km south of the Dugald River deposit (see Xu, 1996; GDA94 z54 coordinates: 410098, 7752960). S_1 is preserved as inclusion trails in D_2-related porphyroblasts (Fig. 4c).

The interaction between D_1 and D_2 is preserved in low-strain domains. A good example is in the north of the mine (North Mine), observable over multiple levels. Here, a large-scale F_1 fold of unknown amplitude is preserved, which is refolded by an F_2 fold. Axial planar S_2, together with bedding and an orthogonal, N-facing joint set create rhomboid blocks (Fig. 5). Bedding-parallel slip has occurred along the bedding planes showing E-plunges, suggesting slip during E-W, D_2 shortening.

3.2.2. D_2 structures

The dominant structural element at Dugald River and the surrounding area consists of a well-developed N-S trending fabric attributed to the regional E-W, D_2 shortening (Newbery et al., 1993; Xu, 1996). D_2 consists of regional to mesoscale, close to isoclinal, N-S trending folds (F_2) and a well-developed axial planar cleavage (S_2). The folding pattern in the Dugald River area has been disrupted during D_4 by the formation of high and low strain domains. Macroscale F_2 folds are well exposed on the surface to the north of the deposit as a series of synform-antiform pairs of tight to isoclinal folds preserved in a D_4 low strain domain (GDA94 z54 coordinates: 411504, 7762204). Within D_4 higher strain domains, F_2 tends to be isoclinal, with synform-antiform pairs disrupted and rootless folds common.

In the northern part of the deposit, F_2 occur as tight isoclinal folds with steep axial planes and north plunges. In the southern part of the deposit, F_2 geometries are more complex with inclined, non-cylindrical folds varying between close to isoclinal (Fig. 6) and having variable plunges towards the north and south.

Associated with the F_2 folds are a series of quartz-carbonate veins that formed through various secondary space accommodating mechanisms during progressive fold tightening (Fig. 6). Tightening of folds is associated with hinge-zone thickening and concurrent limb attenuation. Some veins occur as crosscutting structures along fold limbs and developed in the more competent lithological layers, such as silicified slate beds (Fig. 6b), or as en-echelon veins within beds. Flexural slip along bedding planes in folds has resulted in thin, strike extensive layer-parallel veins (Fig. 6b-c, e-f) and in some isoclinal folds a series of steep, conjugate, and axial planar orthogonal veins formed as well as sub-horizontal quartz-carbonate veins (Fig. 6d), indicating that principal

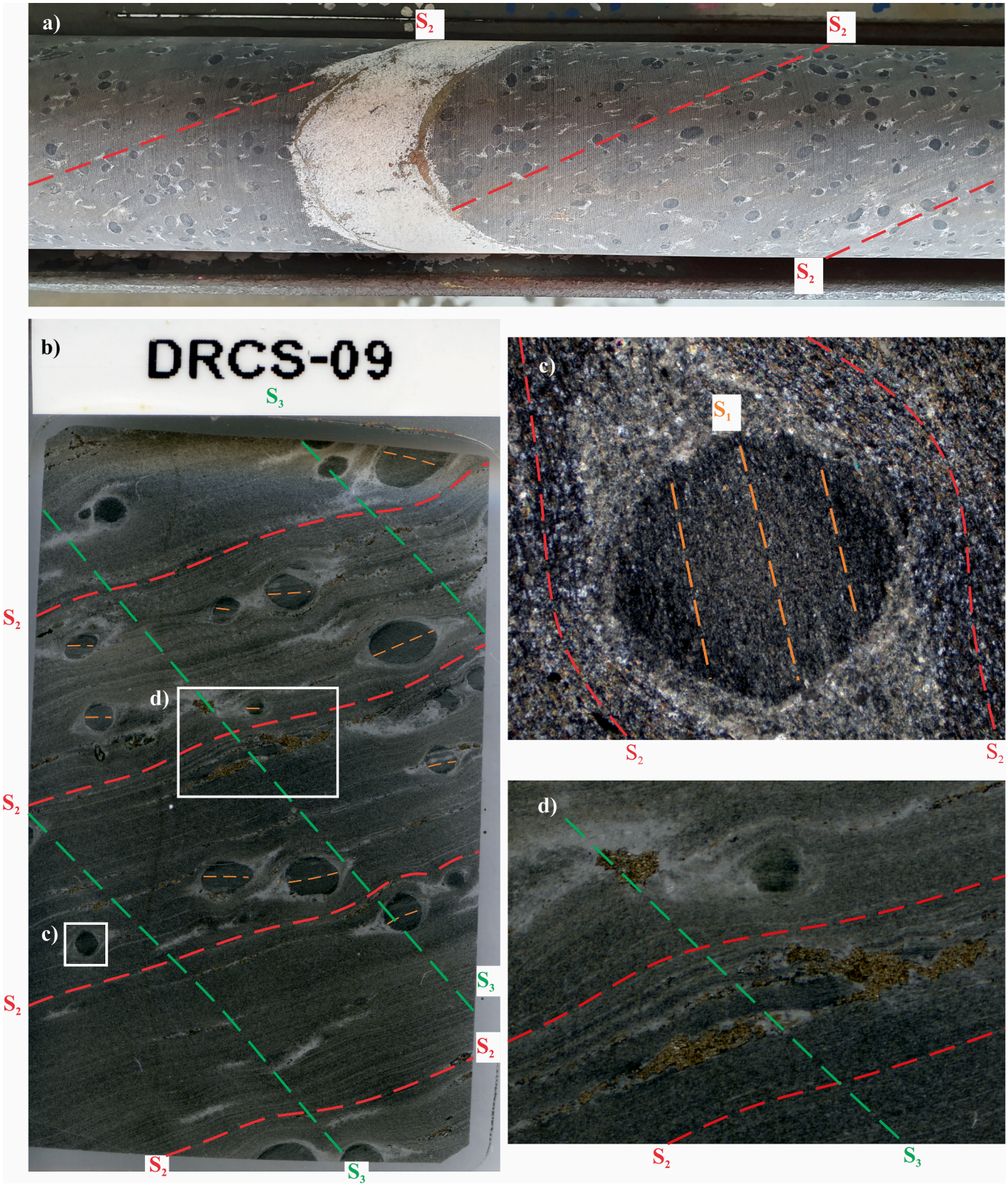

Fig. 4. Low-angle truncation of S_1 (orange dashed lines) preserved in *syn*-D_2 porphyroblasts (dark spots). a) Drillcore (DU2639 – 112.04 m; grid reference 4D) in black slate. Porphyroblasts are aligned parallel to S_2 (red dashed lines) and provide an easily recognisable texture for measuring S_2. Porphyroblasts typically have carbonate-rich strain shadows that are commonly partially replaced by sulphides (typically pyrrhotite). b) High-resolution scan of a polished thin section of (a). In areas of dense porphyroblast development, a crenulation cleavage has developed (S_3; green dashed lines) and has a consistent SW-dip. Porphyroblasts are gently rotated, resulting in S_1 occurring at a low angle to S_2, which itself in this section has formed a composite S_0/S_2 fabric. c) Cross-polarised photomicrograph of the white box in (b) showing low-angle truncation of S_1 inclusion trails by matrix S_2. Reaction rims indicated by strain caps and shadows have increased carbonate alteration. b) Layer-parallel boudinage with pyrrhotite infill in boudin necks.

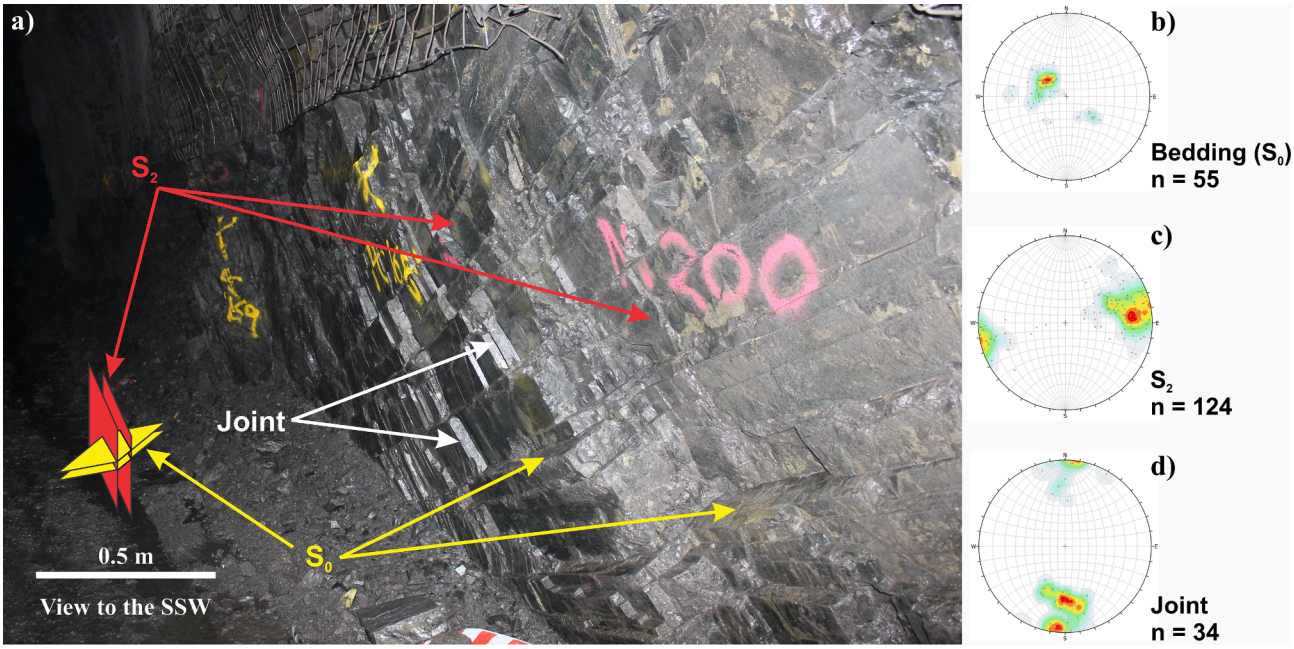

Fig. 5. A) Large amplitude F_1 and F_2 Type 1 interference fold preserved in a low strain domain in the North Mine (grid reference 3B). Here, over successive levels, the interaction of three prominent planes results in the development of rhomboid blocks. Photo was taken in the approximate position of the main shear zone. b, c, d) Equal angle, lower hemisphere stereoplots of S_0 (b), S_2 (c) and joint (d) from levels N125 – N220 (125 – 220 m below surface). S_0 has a consistent southeast dip and small-scale low-angle thrusts are developed within the beds and propagate between them. Steep, S_2 undulates with dominant west dips and is marked by thin, sulphide veins, which combined with the chlorite alteration, causes slabbing along the S_2 planes. The joint set has a general north dip and occurs orthogonal to the bedding.

and intermediate stretching axes are similar (X≈Y≫Z, i.e., prolate strain).

A penetrative S_2 foliation occurs in all rock units. It is generally ~N-S trending with steep, west dips and local east dips due to D_4 (Fig. 7). In slates, it occurs as a slaty cleavage whereas in all the other rock types it occurs as a well-developed schistosity (Newbery et al., 1993, Xu 1996). Pressure solution during D_2 is evident by the development of carbonate strain shadows of porphyroblasts, which themselves are aligned within S_2 (Fig. 4), and strain shadows are commonly partially replaced by sulphides.

3.2.3. D_3 structures

A weak crenulation cleavage (S_3) commonly occurs in the limestone and slate (Fig. 4b). S_3 has a consistent, low-to-moderate southwest dip and is particularly noticeable where high concentrations of porphyroblasts occur in the limestone, causing the localised intensification of S_3 (also Xu, 1996, Spelbrink and George, 2017). The porphyroblasts created a robust layer in which extensional sites in the crenulations were infilled with carbonate-rich material - in effect creating a domainal cleavage in calc-silicate portions of the limestone versus that in relatively more schistose layers.

A top-to-the-E sense of shear is suggested by Xu (1996) and Davis (2017). On the surface, Xu (1996) described F_3 folds with sub-horizontal axial planes, which together with the low-angle S_3 suggests that D_3 had a localised sub-vertical principal stress – a similar observation was made by Davis (2017). At George Fisher mine (Murphy, 2004) and the Monakoff deposit (Davidson et al., 2002) similar observations of flat-lying S_3 crenulations and sub-horizontal F_3 were observed. A possible explanation for this may be a period of orogenic collapse between two major shortening events with co-axial top-to-the-E shearing and referred to as $D_{2.5}$ by Bell and Hickey (1998) and Davidson et al. (2002). While F_3 folds were not directly observed in underground development during this study, the effects of D_3 are apparent in the South Mine as S_0 and axial planar S_2 are locally rotated to moderate southwest dips, which suggest recumbent folding.

3.2.4. D_4 structures

The orebody at Dugald River is truncated by a strike-extensive graphitic shear system that transposed all earlier fabrics. The NNW-ESE trending, anastomosing shear system (the Dugald River Shear Zone; Fig. 3b; see Creus, 2022) is marked by increased graphite and chlorite content compared to the surrounding rock volume. In places, graphite represents a significant concentration, giving the rock a shiny grey, polished appearance and occurring in metre-scale pods. Curvi-planar discrete shear zones within the shear system range from sub-centimetre scale striated fractures that have highly polished, graphitic walls to metre-scale high strain zones with well-developed S-C' fabrics (Figs. 8, 9b). These curvi-planar shear zones link together to form the anastomosing shear system hosting the high-grade mineralisation.

Strain partitioning in discrete shear zones, resulting in pinch-and-swell, is evident over metre scales (Fig. 9). In relatively lower strain domains, which are less than one metre wide, numerous shear bands (C'-planes) can be observed that lie parallel to the shear zone margin. The incipient S-foliation is sub-parallel to S_2 and can be difficult to differentiate given the dark colour of the slates in the shear zone. In high strain domains, which can be several metres wide, a well-developed S-C' fabric has developed. The asymmetry of sigmoidal lenses in the S-C' fabric is consistent with a top-to-the-NE sense of shear during D_4, with an overall oblique-dextral slip (i.e., transpression or the Phase 3 wrench tectonics described by O'Dea et al. 1997). Sigmoidal lenses within the S-C' fabric typically contain a core of sulphide accumulation with wings of graphite-rich material, and within the South Mine, the cores may contain significant sphalerite. Thin mylonites (centimetre scale) occur away from the orebody and are recognisable by the occurrence of highly stretched porphyroblasts.

Transposition in the northern part of the deposit and towards the surface is prominent and resulted in high and low strain domains (Fig. 10a). The high strain domains are marked by the development of S_4 that transposed earlier fabric with rootless F_2 folds often observed. Due to the co-planarity of D_2 and D_4, S_4 is observed sub-parallel to S_2 and can be difficult to differentiate. Low strain domains preserve F_2 folded S_0

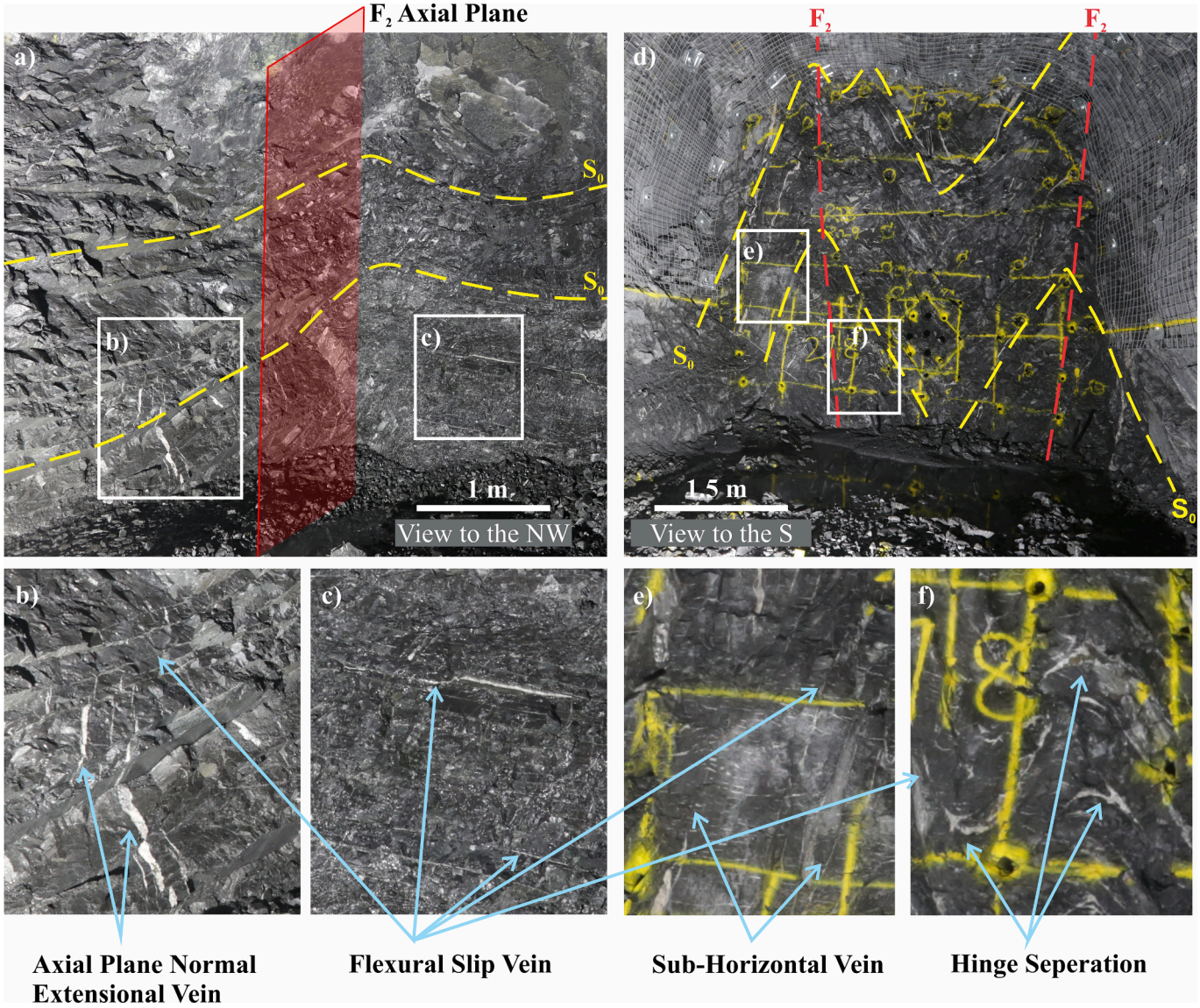

Fig. 6. F_2 folds in the South Mine. Folds are open (a) to close (d) with folds away from the ore body typified by lower angle eastern limbs (a). Several space accommodating mechanisms resulted in the development of quartz-carbonate veins (b-c, e-f). Hinge separation occurs where folds are close to isoclinal (f; also Fig. 13f, Fig. 14a).

and quartz-carbonate veins developed during fold tightening.

D_4 cleavages occur as zones of crenulation cleavage and transposed fabric observed at the microscale. Domanial cleavages commonly result in preferential development of late D_4 cleavages in favourable bands such as micaceous bands. In slates proximal to the ore body, strain partitioning into biotite-rich layers resulted in the development of a composite $S_{2/4}$ foliation, whereas in graphitic layers a crenulated cleavage is observed with S_4 micro-folding S_2 in lower strain domains of F_2 hinges.

Rare folding at the contact of limestone and slate can be attributed to D_4 with black porphyroblasts, that are aligned parallel to S_2, providing evidence of post-D_2 folding. The outcrop-scale folds are disharmonic and contain carbonate-infilled fold-accommodation faults within the fold hinges. Axial planes are moderate, E-dipping and have moderate northwest plunges and rare southeast plunges.

3.2.5. *D_5 structures*

The final major deformational event to affect the Dugald River deposit is associated with the reactivation of earlier shears and faults (Fig. 10), as well as the development of small-scale shears within thicker ore bodies and D_4-related tension gashes. Reactivation of shears resulted in the development of incohesive fault rocks (Fig. 10c) and metre-scale displacement of ore lenses and limestone/slate contact zones. Offsets are particularly noticeable along SW-dipping shear/fault planes. Generally, steeper structures tend to display cataclasis and low-angle structures display brecciation, particularly along the footwall. Near the limestone contact, the reactivated low-angle thrusts typically involve a damage zone with quartz-carbonate infill and may have chlorite alteration.

The wings of sigmoidal lenses within the S-C' fabric were mechanically sheared leaving the cores as well-rounded clasts within the cataclastic zones with a matrix of graphite-rich brecciated carbonate, quartz and sulphide (Fig. 9c). Striations on fault-walls are ambiguous with both strike-slip and dip-slip vectors recorded and cannot be attributed to D_4 or D_5, however, kinematics largely indicate a dextral sense of shear.

3.2.6. *Metamorphism*

The stratigraphic sequence contains abundant garnet and scapolite porphyroblasts which indicate that the minimum P-T conditions reached upper greenschist to lower amphibolite facies. According to Foster and Rubenach (2006) and Whittle (1998), peak metamorphism at Dugald

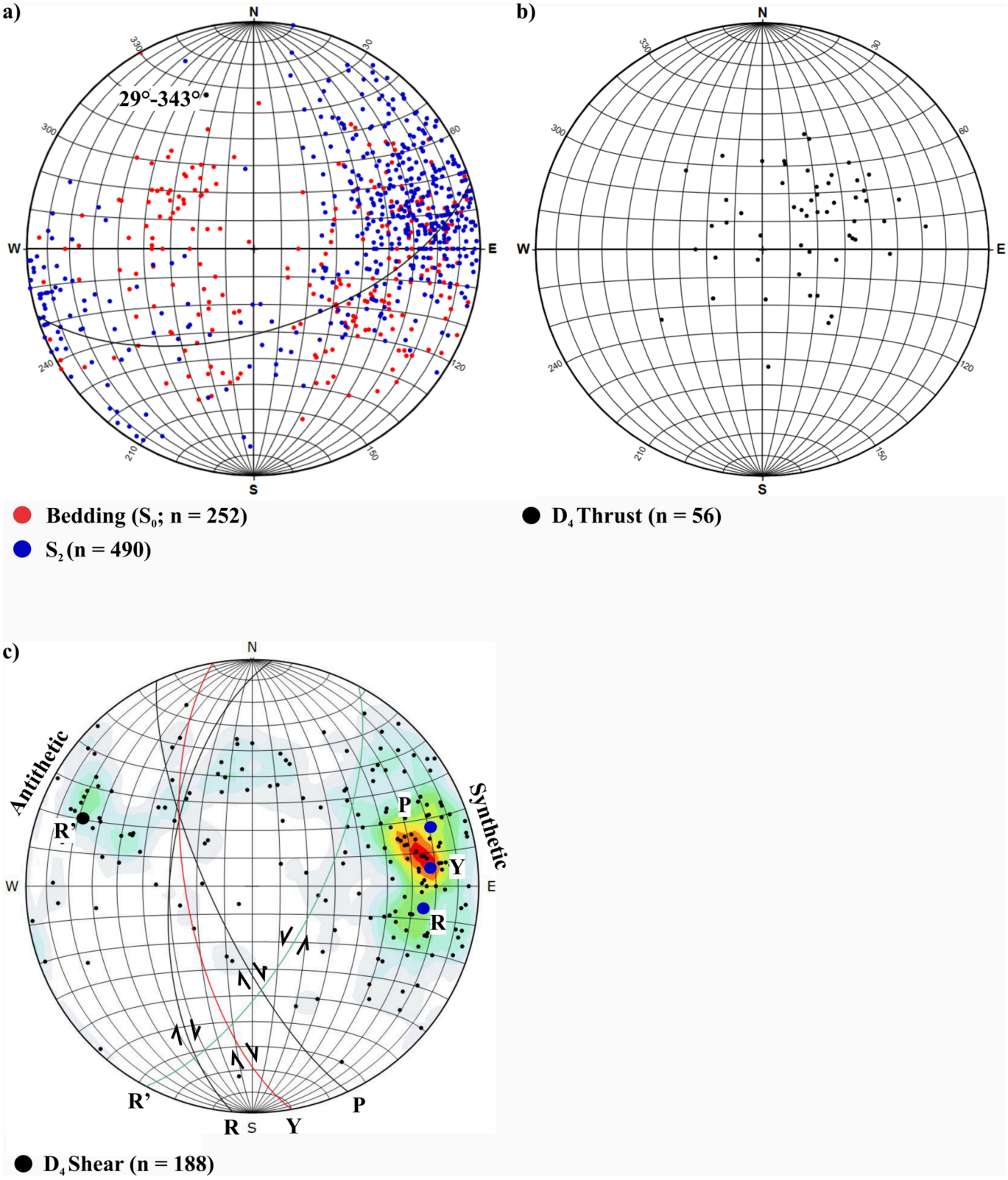

Fig. 7. Equal area, lower hemisphere stereoplots for poles to planes. a) The planar fabric at Dugald River is NW-SE trending with dominant WSW dips due to east verging folding during D_2. Low strain domains of D_4 preserve F_1 and F_2 Type 1 interference folds highlighted by the SE- and NW- dipping bedding (S_0) b) SW-dipping zones of S_3 intensification were reactivated early D_4 as thrusts with a top-to-the-NE sense of shear. c) The Dugald River Shear Zone developed as a dextral Riedel shear network with both synthetic and antithetic structures developed.

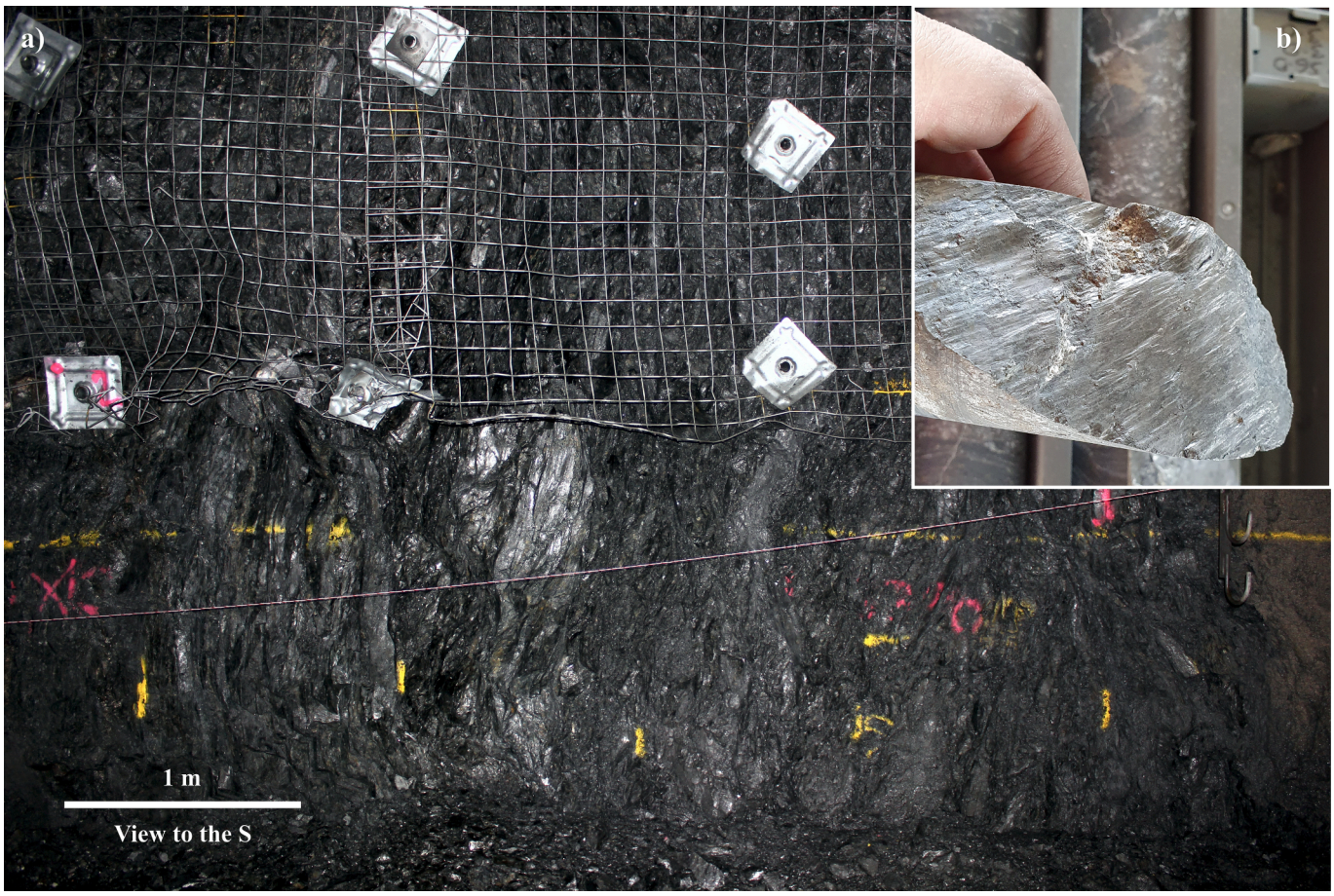

Fig. 8. Characteristic range of discrete shears within the Dugald River Shear Zone. The shear zones are marked by increased graphite and chlorite. a) Metre-scale high strain zones are common in the South Mine (grid reference 4E) and marked by a well-developed S-C' fabric that has been a focus for D_5 brittle reactivation. b) Thin, shears with highly polished walls that are typically striated. Notably, a discrete structure can commonly pinch from a metre-scale high strain zone to a sub-centimetre shear.

River may have reached mid-amphibolite facies (Fig. 2). Foster and Rubenach (2006) placed the host sequence at Dugald River in a belt that they assigned to the diopside zone. Moreover, staurolite- and sillimanite-bearing rocks have been described from the coarse-grained mica schists that occur west of the deposit implying temperatures of up to 600 °C (Whittle, 1998). Calcite grains analysed by George (2011), associated with the carbonate-slate contacts, have MgO-contents up to 2.7 wt% equivalent to 7 mol % $MgCO_3$. Metamorphic calcites with this composition can only be stable at temperatures >600 °C (Anovitz and Essene, 1987) and is the only petrological indication that the metamorphic grade of the Dugald River Slate may be as high as recorded in the mica schists that occur to the west of the deposit. A detailed metamorphic study is recommended for the deposit.

4. The Dugald River shear zone

The Dugald River Shear Zone is a NNW-trending structure situated to the east of the Knapdale Quartzite within the Mount Roseby Schist (Fig. 3b; see Creus, 2022). The surface expressions of the shear zone include a 5 m thick Zn gossan that is approximately 2.5 km long and disappears under cover along strike. At depth, the shear zone was intercepted by drilling at 1 km below the surface.

At the deposit scale, the shear zone has an overall sigmoidal geometry, dipping at 40°−90° to the west (Fig. 11). In the North Mine, the shear zone is steeper compared to the South Mine and has localised east dips. In the South Mine, at ~290 m below the surface, the dip of the shear zone flattens and steepens again at depth (Figs. 11, 12b). This change in dip from steep to moderate and back to steep manifests as a pronounced flexure zone in the geometry of the shear zone. The thickness of the shear network is related to the dip angle of the shear zone: where the dip is steeper, the shear zone is thinner, and conversely, where the dip is at a lower angle the shear zone is wider.

The shear zone is characterised by anastomosing shears and fractures that reflect a fractal pattern. The geometry of metre-scale shears which locally comprise well-developed S-C' fabric is reflected in the large-scale geometry of the shear zone. Discrete shear planes within the shear zone can be traced, and modelled, based on drill logging and underground face and drive mapping, including digitised shear planes from Structure-from-Motion – Multiview Stereo (SfM-MVS) photogrammetry (Creus et al., 2021).

In the South Mine, moving towards the west (grid reference on Fig. 3: 4C and 4D), several shear zones occur at a variety of scales and are separated by lower strain zones that may preserve D_2-related fabric elements, thereby creating an anastomosing system of high strain zones bounding lower strain domains. Furthest west, a mine-scale shear (light green polyline on Fig. 3b and purple surface on Fig. 12) bifurcates from the principal displacement zone (purple polyline on Fig. 3b and red surface on Fig. 12) at grid reference: 4D. The shear merges with the principal displacement zone in the north at grid reference 3A. In the North Mine, where the shear system is steep and sub-parallel to the pervasively developed S_2, fewer discrete shears are splaying off the principal displacement zone and they tend to terminate into S_2 within a few metres.

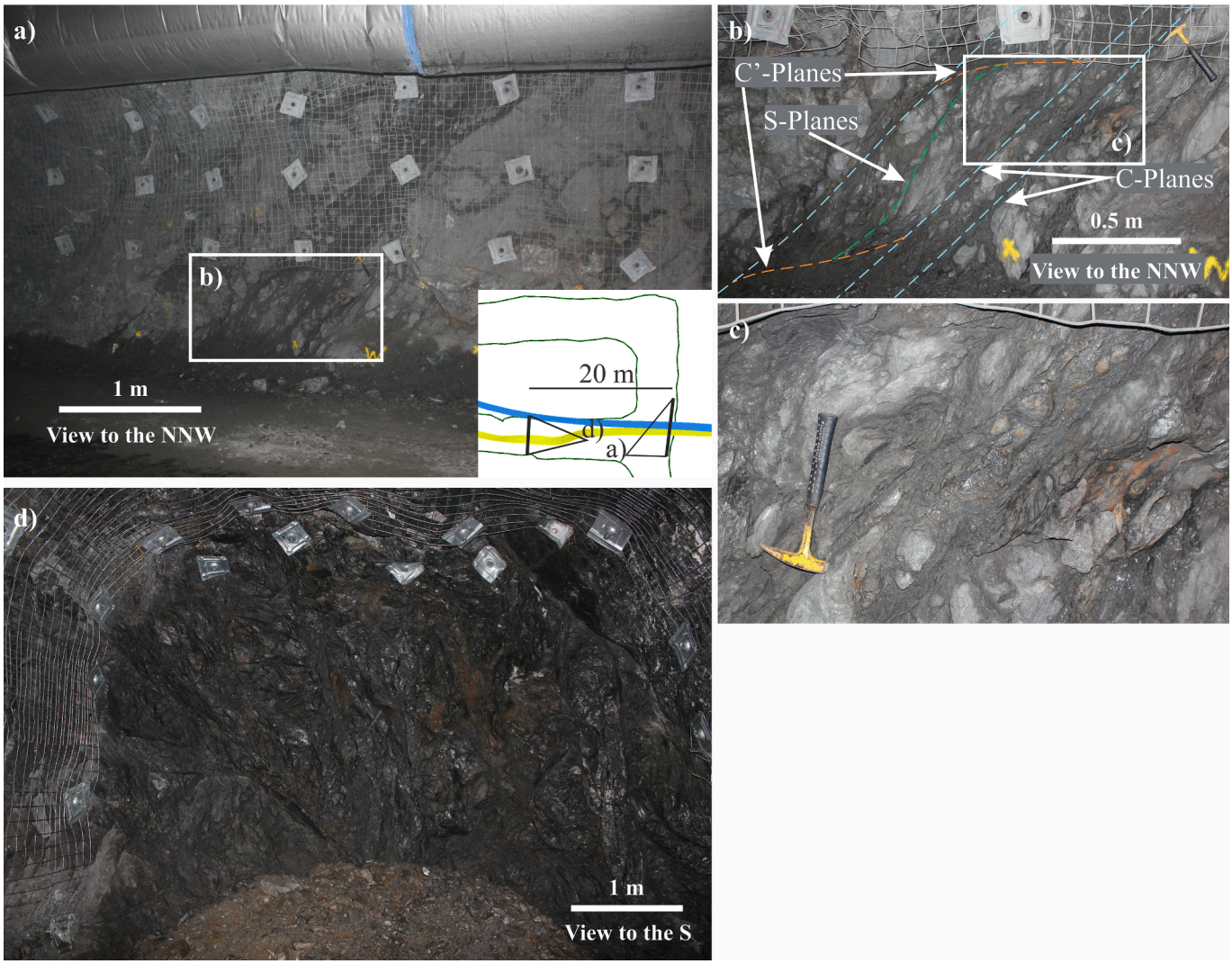

Fig. 9. Example of pinch and swell of a discrete shear within the Dugald River Shear Zone (grid reference 4D). a) and d) occur 20 m along strike (see insert in a). The yellow and blue planes in the insert are the footwall and hangingwall of the shear zone, respectively. a) Shear zone, while narrower displays a well-developed S-C' fabric (b and c; geopick for scale) that has been reactivated during D_5 to form an incohesive cataclasite with rounded sigmoidal lenses. d) Here the shear zone is thicker with thinner discrete shears that are sympathetic to the shear zone.

4.1. Riedel shear network

The Dugald River Shear Zone developed as a Riedel shear network (see Creus, 2022). Riedel shears develop with distinctive geometric arrangements and are given different names based on their kinematics and orientations (i.e., R, P, R', P', Y and T; Riedel, 1929; Tchalenko, 1968; Naylor et al., 1986; Davis et al., 2000). Idealised models for Riedel shear networks propose that strike-slip movement within a basement fault is propagated into flat-lying, relatively homogenous cover sequences where strike-slip shear strain is imposed, with slip surfaces developing in distinctive geometries (Fig. 12c). Field-based studies of Riedel shear networks suggest that basement faults are not necessary for Riedel shears to develop (e.g., Davis et al., 2000; Mueller, 2020) and may also develop in inclined to steep dipping strata (Swanson, 2006; Dirks et al., 2009; 2013; Mueller, 2020).

Riedel shears develop en-echelon and stepwise, and at Dugald River, R-, R'-, P- and Y-shears have been recognised. The first Riedel shears to develop are R-shears, which are synthetic to the shear direction and develop at ~15°, clockwise to the shear direction. R'-shears developed within overlap zones of R-shears and are antithetic to the shear direction and occur at ~75°, clockwise to the shear direction (Davis et al., 2000). With increasing strain, P-shears develop at ~15°, anticlockwise to the shear direction. Finally, as the R- and P-shear segments grow, they interconnect to form throughgoing Y-shears, which at Dugald River is responsible for the anastomosing pattern of the Dugald River Shear Zone (see Creus, 2022).

5. Ore body geometry and textures

5.1. Ore body geometry

The elevated Zn-grades that define the Dugald River ore body have a close spatial relationship with the Dugald River Shear Zone (Fig. 3b, Fig. 12). The ore body, defined by the Inferred resource volume, consists of a ~2.5 km, NNW-trending continuous major ore body and several smaller bodies to the west that are hosted within, and parallel to the shear zone. The main ore body has been intersected to a depth of 1 km below the surface and potential remains to the north, south and at depth. The mineralisation is orientated at a low angle relative to the stratigraphy (Fig. 12b). At depth in the South Mine, mineralisation is proximal to the contact between the calc-silicate and slate. Towards the surface and the North Mine, mineralisation gradually shifts towards the contact with the limestone and slate. The gradual shift is marked by a flexure and thickening of the deposit, which represents an oblique dextral step-

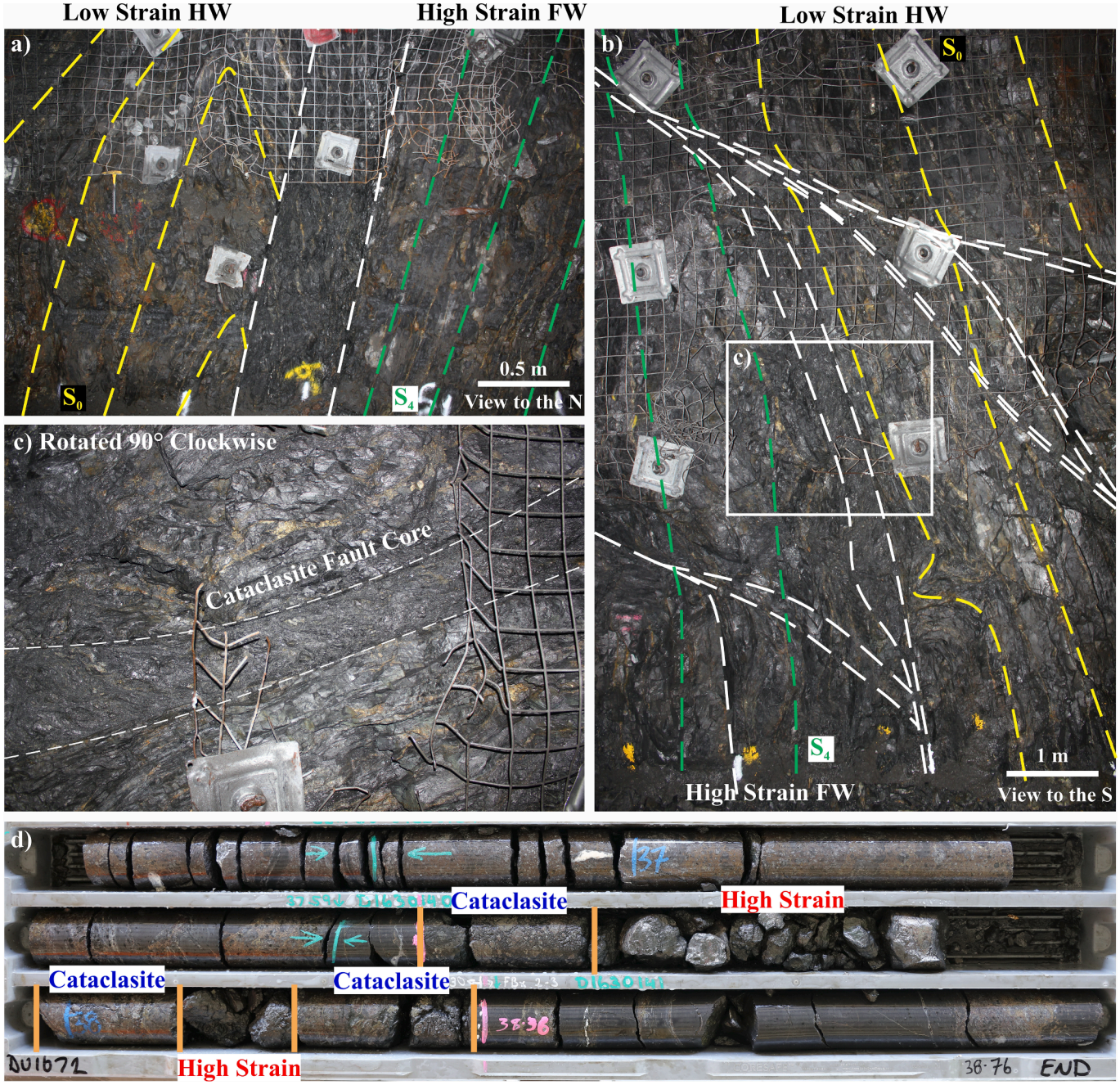

Fig 10. Strain partitioning during D_5 resulted in variable development of fault rocks. a) and b) are outcrop expressions of a reactivated part of a mine-scale shear and are on opposite sides of S150_XC423_W (grid reference: 4C). a) The northern side of the drive shows that the high strain character of the D_4 shear is still recognisable as an S-C' fabric. Note, the D_4 related truncation of F_2 folded bedding (S_0) in the hangingwall (HW) of the principal displacement zone. In the footwall (FW) of the principal displacement zone, S_0 is no longer distinguishable from S_2 and transposition has occurred with boudinage of sulphide veins common. b) In the southern side of the drive, the S-C' fabric has been mechanically sheared to form incohesive cataclasite (c; note image is rotated 90° clockwise). d) Drill-core example of a reactivated shear, which includes high-grade matrix breccia texture that typically maintains cohesion as opposed to relatively more graphite-rich parts of shear zones.

over in the shear zone (i.e., a releasing bend). In addition, subordinate ore bodies bifurcate from the major ore body at the flexure.

Individual ore bodies typically occur along the footwall of major Y-shears (e.g., Fig. 3b, Fig. 12). In addition, the geometry of the shear zone and thickness of the ore body has a direct relationship: where the shear zone is steep and thin, the ore body is steep and thin whereas, where the shear zone has a lower dip angle and thickens the ore body is thicker and has a lower dip angle.

5.2. Ore textures

The geometry of the ore zone parallels the Dugald River Shear Zone and has an apparent tabular shape (Fig. 12). The ore textures (Fig. 13) vary along the ore zone and can be categorised into breccia and planar ore (e.g., Newbery et al., 1993; Xu, 1996; Spelbrink and George, 2017). The remainder of this section is a summary of Newbery et al. (1993), Xu (1996), Spelbrink and George (2017) and observations during this study. The breccia ore represents the most economic style of mineralisation, highest grade and thicker ore zones, and is particularly abundant in the southern end of the deposit where the ore body is thicker and has a

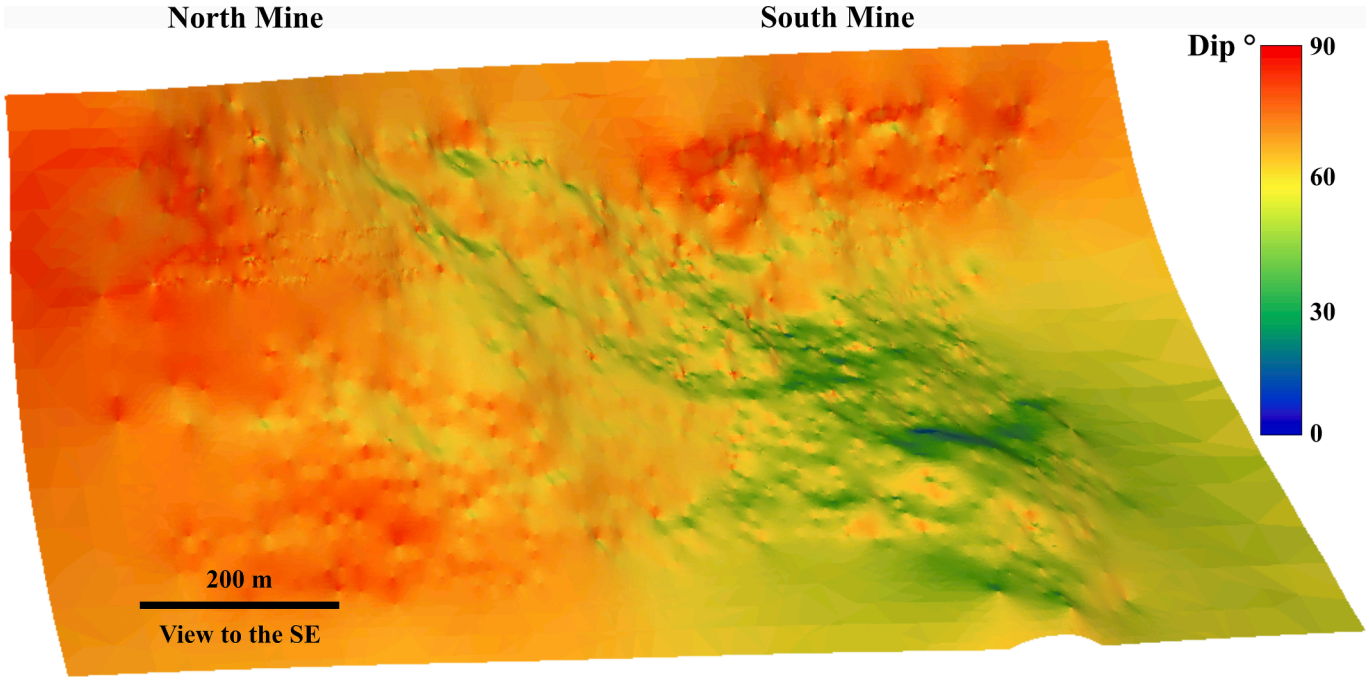

Fig. 11. Wireframe triangle faces of the principal displacement zone colour coded according to dip angle. The shear zone in the South Mine is marked by a flexure with moderate dips to the southwest. Towards the north and surface, the shear zone steepens and in the North Mine, local east dips occur.

lower dip angle, while planar ore is abundant in the northern end of the deposit where the ore body is thinner and has a sub-vertical dip (Fig. 13a).

End-member types for the breccia ore texture include clast supported and matrix-supported. The clast supported breccia is characterised by centimetre- to metre-scale sub-angular clasts of slate and sub-centimetre clasts of quartz and pyrite in a matrix dominated by sphalerite, however other matrix sulphides include pyrite, pyrrhotite and galena. Clasts of folded slate are common and the presence of an axial planar cleavage in some of the clasts indicates that the shearing occurred after the main folding event. Most slate clasts contain bedding parallel carbonate veins and veinlets that are partly to completely replaced by sulphides, mainly sphalerite (Fig. 13e). The matrix-supported breccia is characterised by variably sized, rounded slate, pyrite, quartz and rare fluorite clasts (Fig. 13b) in a fine-grained matrix of sphalerite with subordinate amounts of galena, pyrite and pyrrhotite. Clasts rarely exceed 10 cm in length. In the South Mine, where the ore body thickens, the footwall to the ore body consists of a thick zone of carbonate matrix-supported breccia with trace amounts of pyrite, sphalerite, pyrrhotite and galena (Fig. 13b). Locally, pyrrhotite-rich matrix-supported breccia occurs and is associated with a pronounced drop in the Zn grade and the appearance of visible chalcopyrite. The pyrrhotite-rich breccia is usually fine-grained and displays evidence of shearing and appears to overprint the earlier sphalerite-rich breccia (e.g., Fig. 13g).

Planar ore textures are common in the northern part of the deposit and include banded and stringer ore. Banded ore consists of alternating bands of sulphides and black slate (Fig. 13d). The sulphides occur as both fine-grained crystals and coarse-grained annealed aggregates, suggesting replacement and remobilisation during deformation. Some clasts within the breccia ore consist of banded type ore suggesting that the banded ore predates the breccia ore.

Stringer ore represents a widely distributed ore texture usually occurring along the periphery of breccia type ore. The stringers have variable thicknesses and commonly occur as a series of bands that are sub-parallel to the S_2 fabric, suggesting that this ore type may represent replacement ore of the S_2 fabric or D_2 carbonate veins. The main sulphide phases within the stringer ore are sphalerite and pyrite with subordinate pyrrhotite and rare galena.

In general, the ore textures have a zonation pattern that appears to correlate with the geometry of the ore body/shear zone (Fig. 13a). In the North Mine where the ore body is steep, ore textures are dominated by planar ore with thin, discontinuous lenses of breccia ore. Towards the south, where the ore body has a lower dip angle, breccia type ore dominates and weaves around planar ore.

5.3. *Boudinage*

Sulphide accumulation into dilational sites created by boudinage is common within the deposit (Fig. 4d, 14; Davis, 2017). Layer-parallel boudinage of attenuated limbs of tight to isoclinal F_2 folds is common and boudin necks are characteristically cross-shaped and infilled with quartz-carbonate, which has subsequently been replaced by sulphides during mineralisation. Foliation boudinage is a possible mechanism for the cross-shaped boudin necks given the lack of rheological contrast within the slate (Fig. 14d–e; e.g., Aerden, 1991; Arslan et al., 2008; 2012). Infill of pyrite, pyrrhotite and sphalerite in boudin necks combined with a lack of deformation of the sulphide grains suggests precipitation coeval with boudin formation (Davis, 2017). However, it should be noted that while boudin necks contain sulphides, the arms of boudins are typically comprised of quartz-carbonate suggesting the replacement of carbonate by sulphides (Fig. 14e). Torn boudins are common in the planar ore and larger clasts of the breccia ore (Fig. 14a–c). Here the slate layers, which are competent layers enveloped by sulphides resulted in strain rate incompatibilities which caused layer extension, resulting in angular, block-shaped boudins with necks infilled by sulphides.

5.4. *Ore paragenesis*

Microscale and hand-specimen analysis of high-grade breccia ore indicate that there were at least two main phases of sulphide mineralisation. The first phase is associated with the replacement of carbonate in quartz-carbonate veins during late D_2, and the second phase is associated with intense brecciation during D_4 with associated quartz-carbonate fluid injection.

Observations of D_2-related mineralisation, herein referred to as

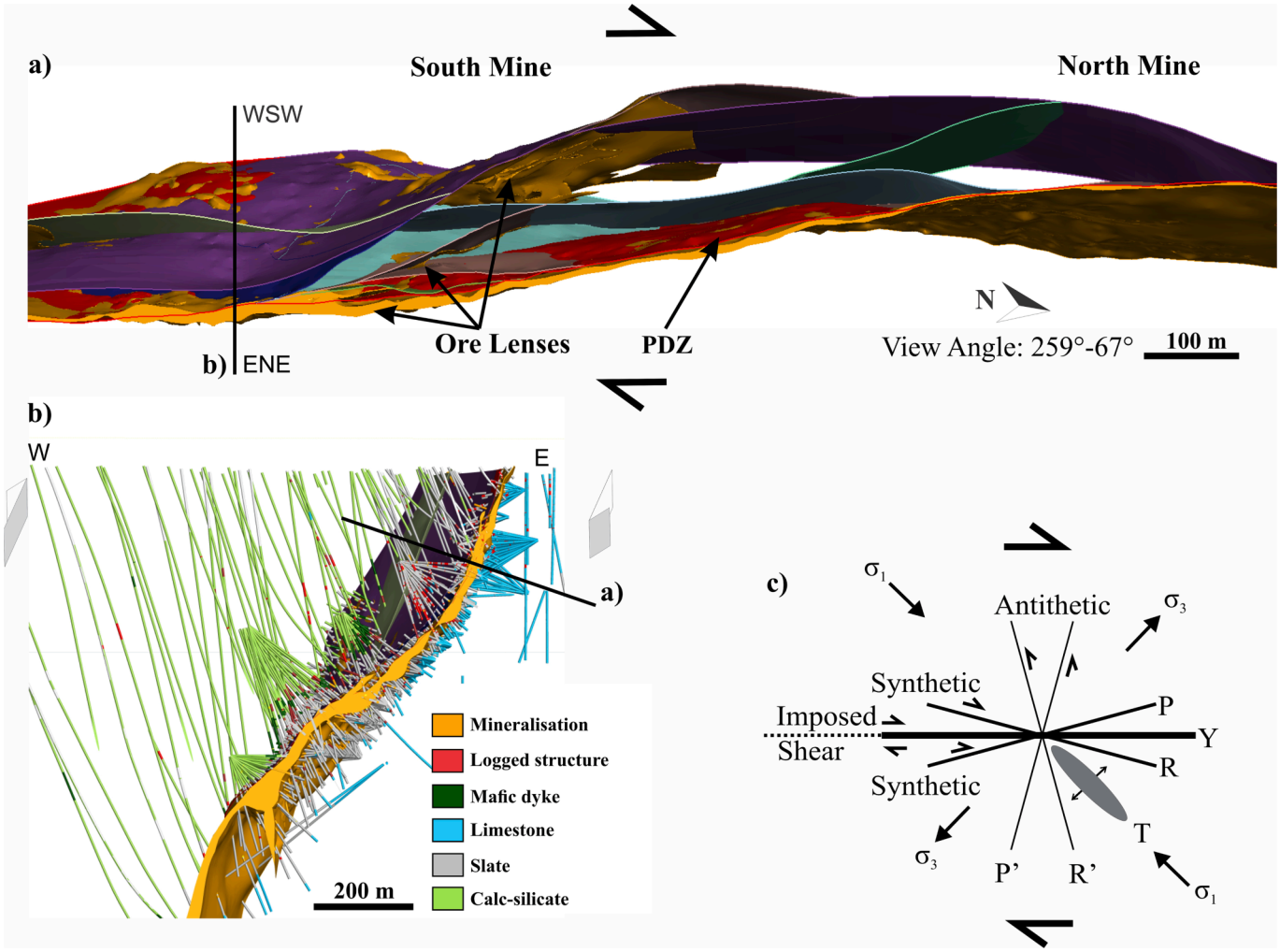

Fig. 12. A) down-dip overview of the Dugald River Shear Zone and high-grade Zn volume (>7% Zn). The shears bifurcate and merge to form an anastomosing shear zone with an oblique dextral sense of shear. Note the thinning of the mineralisation towards the north and the surface. b) Cross-sectional view looking north through the South Mine. The location of the cross-section is shown in (a). c) Schematic representation of Riedel shears developed within a dextral, compression strike-slip shear zone.

Phase 1 mineralisation, under the microscope and at outcrop-scale indicate that during this phase, pyrite was the dominant sulphide species with significant sphalerite and minor galena and pyrrhotite. Pyrite, sphalerite and galena crystals are preserved as rounded clasts in breccia ore and are typically coarse-grained.

During the second phase of mineralisation, herein referred to as Phase 2 mineralisation, sphalerite was the dominant sulphide species together with significant pyrite and galena. Episodic injection of sulphide-rich fluid is indicated by the variable grain size of matrix sphalerite, and the observation that in many rounded clasts of D_2-related veins, the clasts are surrounded by fine-grained polycrystalline quartz and inclusions, some of which are sulphides. In general, where finer-grained matrix sphalerite occurs the number of rounded clasts is greater. Pyrrhotite is inferred to have precipitated late during D_4, but at a time when the sulphides were still ductile as indicated by sheared pyrrhotite within matrix-supported sphalerite breccia (e.g., Fig. 13g). It appears that away from the orebody, pyrrhotite is the dominant sulphide and tends to infill micro-fractures in slates and limestone. Furthermore, selvedges of pyrrhotite are stretched and dismembered into smaller segments, parallel to S_2 and S_4.

6. Discussion

The close spatial–temporal relationship between the Zn-Pb mineralisation and the Dugald River Shear Zone suggests that the Dugald River deposit can be classified as an epigenetic, shear zone hosted deposit. While the data presented in this publication indicate a strong structural control on the development of the deposit in its current setting, the question remains whether or not precursor mineralisation existed and if so, was it initially in a SEDEX or diagenetic environment as proposed for other deposits in the Mount Isa Inlier and McArthur River areas (e.g., Newbery et al., 1993; Dixon and Davidson, 1996; Large et al., 2005; Spinks et al., 2020; Rieger et al., 2021). For example, the banded ore texture (*viz.* planar ore, Fig. 13a), common in the North Mine, was used to argue for a genetic model of early, syngenetic or diagenetic, stratabound mineralisation with a later hydrothermal overprint (Newbery et al., 1993; Dixon and Davidson, 1996). Newbery et al. (1993) suggested that the laminations in the banded ore represent sedimentary layering and the layers containing equant grains of sulphides indicate uniform recrystallization and limited remobilisation, whereas the coarse-grained, sulphide-rich bands represent remobilisation and recrystallization during deformation. Dixon and Davidson (1996) argued that the fine-grained pyrite that occurs as "minute" subhedral grains enclosed by anhedral sphalerite and pyrrhotite indicates that the base-metal sulphides were introduced after the growth of the pyrite within the sediment. Furthermore, they suggest that high δ^{34} sulphur in sulphides was inherited from a component of earlier diagenetic sulphur and that the limestone acted as an impermeable layer

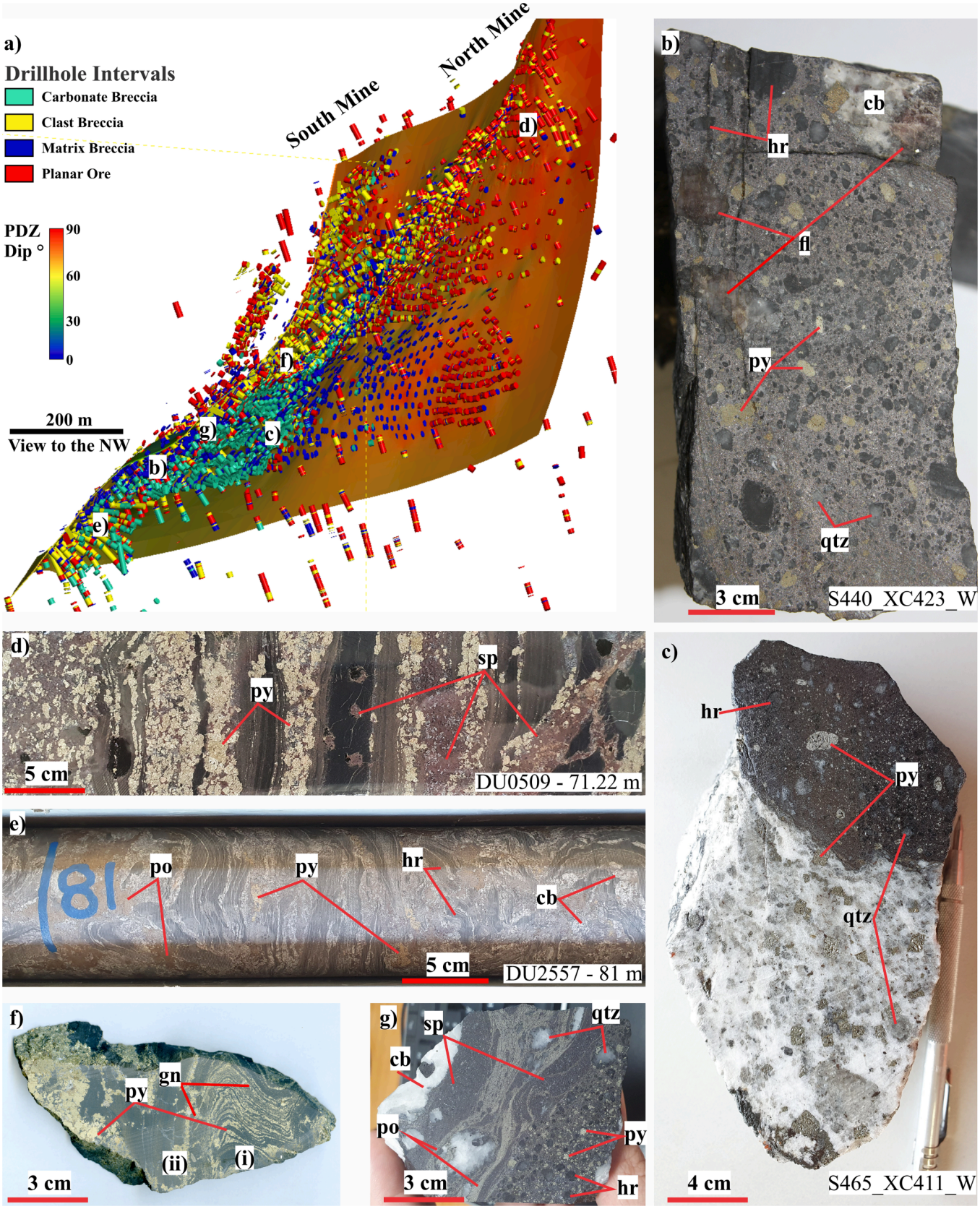

(caption on next page)

Fig. 13. Main ore textures observed in the Dugald River deposit. a) Oblique section through grid reference 4D and the "back" of the section showing the distribution of the main ore textures as colour coded drillhole intervals. The footwall plane of the principal displacement zone (PDZ) is coloured according to the wireframe triangle face dip. b) High-grade matrix-supported breccia that is dominant in the South Mine. Here the matrix comprises sphalerite (sp) and minor pyrrhotite (po). c) Carbonate breccia forms an eastern zone of low-grade mineralisation and is only found in the South Mine and represents a quartz-carbonate brecciation front that was replaced by sulphides. In this sample, the rounding effect due to sulphide remobilisation of competent wall-rock, including pyrite (py) is highlighted. In the carbonate breccia, the pyrite is largely euhedral. d) The North Mine is dominated by transposed sulphide veins that are parallel to S_2 and form the planar ore. e) Clast supported mineralisation is found throughout the deposit – mainly in the South Mine - and is marked by clasts of D_2 related folds. Folded clasts often contain thin veinlets of bedding parallel carbonate veins that are partially to completely replaced by sulphides. f) Hand-scale example of a tight fold where flexural slip along bedding planes has resulted in veining. With fold tightening sulphides migrate into extensional sites such as fold hinges (saddle reefs; (i)) and boudin necks (ii). Pyrite grains in the flexural slip veins, boudin necks and hinges are fine-grained, whereas, in S_2 parallel veins, pyrite is coarse-grained. g) Post-breccia shearing can develop in matrix-supported breccia as pyrrhotite bands within fine-grained sphalerite. The pyrrhotite bands can be thicker and contain rounded fragments of wall rock, quartz and fluorite. Abbreviations: pyrite (py), sphalerite (sp), host rock (hr); quartz (qtz), fluorite (fl), carbonate (cb), pyrrhotite (po), galena (gn).

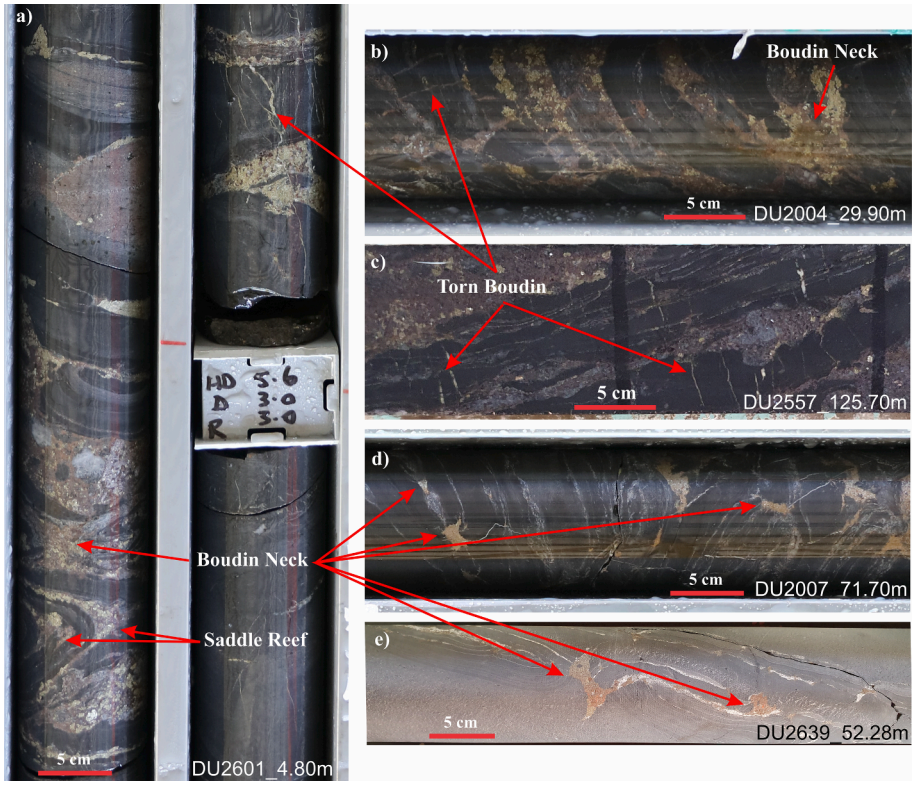

Fig. 14. Common boudinage patterns observed at Dugald River where boudin necks are generally infilled with sulphides. a) Hinge separation of a close fold with infill of sulphides to create a saddle reef which in this instance is infilled with coarse-grained pyrite and fine-grained sphalerite. Adjacent to the saddle reef is cross-shaped boudin necks infilled by coarse-grained pyrite and fine-grained pyrite. a, b, c) Torn boudins with sulphide infill in the necks occur where thicker (centimetre-scale) slate layers are enveloped by sulphide layers. d, e) Foliation boudinage within slate (e) and limestone (d).

trapping Zn-Pb brines within the slate package.

We suggest that the banded ore represents quartz-carbonate-sulphide veins that developed within the black slate and were progressively flattened, attenuated, dismembered, and transposed into parallelism with S_2 (Fig. 13d). During progressive deformation, the veins were boudinaged as they were rotated into parallelism with S_2, and the boudin necks acted as dilational sites where pyrite, sphalerite and galena migrated and crystallised. Although, the Dugald River deposit is completely shear zone hosted we cannot exclude the possibility of early syngenetic or diagenetic mineralization that was subsequently upgraded during deformation and continuous tectonism. In the following section we propose a structural model for the formation of the Dugald River ore deposit based on detailed mapping, core logging and 3D modelling of the ore body and structures.

Our observations indicate that the Zn-Pb mineralisation at the Dugald River deposit is hosted within the Dugald River Shear Zone and the sulphide mineralisation comprised at least two depositional phases. The first phase of sulphide deposition involved transport in hydrothermal/metamorphic fluids and is represented by mineralisation hosted in *syn*-D_2 quartz-carbonate veins. The second and the main phase of sulphide deposition involved a combination of fluid-assisted transport and mechanical remobilisation and is represented by the breccia, planar and the stringer ore hosted by the D_4 Dugald River Shear Zone.

6.1. *Sulphide mobility during hydrothermal and deformation events*

Sulphides undergoing deformation and metamorphism can be mobilised by fluids and by solid-state deformation, often both processes occurring simultaneously which is referred to as mixed-state solution (e.g., Hobbs, 1987; Marshall and Gilligan, 1987; 1989; 1993; Marshall et al., 2000; Tomkins, 2007; Zhang et al., 2014). Mechanical remobilisation (i.e., solid-state solution) involves a process of translocating sulphides from zones of high mean rock stress to zones of lower mean rock stress during ductile deformation (e.g., Tomkins, 2007). Usually, this process involves the migration of sulphides from fold limbs to hinge zones (e.g., Marshall and Gilligan, 1987; Tomkins, 2007) and the same principle applies to dilational jogs in shear zones and boudin necks.

According to Tomkins (2007), mechanical remobilisation is effective at redistributing massive sulphides as they act as single units that are more ductile than the surrounding silicate rocks. In this manner, sulphides can be remobilised on the scale of 10′s metres when compared to the movement of disseminated ore, which occurs on the scale of centimetres (Marshall et al., 2000; Tomkins, 2007; Zhang et al., 2014). Experimental results indicate that sulphides undergoing deformation

have a strength order, *viz.*, galena (weakest) < chalcopyrite < pyrrhotite < sphalerite < pyrite (strongest) with the middle 3 interchangeable (Marshall and Gilligan, 1987). Furthermore, all sulphides but pyrite undergo several deformation processes starting from greenschist facies and include ductile deformation, solid/liquid state remobilisation and annealing (Craig et al., 1998). At higher metamorphic grades, i.e., at amphibolite facies and higher, massive sulphides tend to migrate as a whole with little mechanical fractionation of the ore (Tomkins, 2007). The relative strength between different sulphide phases also has a bearing on the preferential remobilisation of metals within the sulphide horizons (Marshall and Gilligan, 1987).

The breccia ore represents the highest grade of mineralisation, particularly the matrix-supported breccia. Rounded clasts of wallrock, vein quartz-carbonate, fluorite, and pyrite are inferred to have formed through the process of mechanical remobilisation. Initially, competent rock fragments (including pyrite and quartz-carbonate veins) cracked through brittle deformation (e.g., cataclasis) with ductile sulphides migrating into the cracks, forming the clast-supported breccia (e.g., Fig. 15). The competent fragments were mechanically deformed through kneading, milling and rotation to form the matrix-supported breccia as the massive sulphide horizon thickened. This process is often referred to by the German term "durchbewegung" first described by Vokes (1963) and further discussed by e.g., Maiden et al. (1986), Klemd et al. (1987), McQueen (1987), Cook et al. (1993) and Zhang et al. (2014). Durchbewegung is an internal feature of ore deposits and is the result of intense progressive simple shear within fault and shear zones (Marshall and Gilligan, 1987) with two endmembers described (e.g., Maiden et al., 1986; Klemd et al., 1987; McQueen, 1987):

1. Progressive fold tightening to isoclinal folds where alternating layers of silicate rocks and massive sulphides become disrupted and separated, with the migration of sulphides between the silicate clasts, which includes disrupted folds and boudins. The clasts then undergo rotation within the sulphide matrix.
2. Progressive brittle fracturing of competent wall rock at the interface with a sulphide horizon results in the migration of sulphides into the fractures, and wall rock clasts are incorporated into the sulphide matrix and rotated.

6.2. *Phase 1 mineralisation*

Phase 1 mineralisation marks the first evidence for mineralisation and occurs during late D_2, following quartz-carbonate veining and peak metamorphism and is inferred to have been sub-economic. Underground mapping and core logging of structures, veins and mineralisation textures allow for the reconstruction of progressive, ductile deformation and mineralisation during D_2 (Fig. 16). D_2 folds become tighter proximal to the Dugald River Shear Zone which resulted in the progressive steepening of veins, parallel to S_2, followed by boudinage and the coalescing of veins and boudin necks. The formation of quartz-carbonate

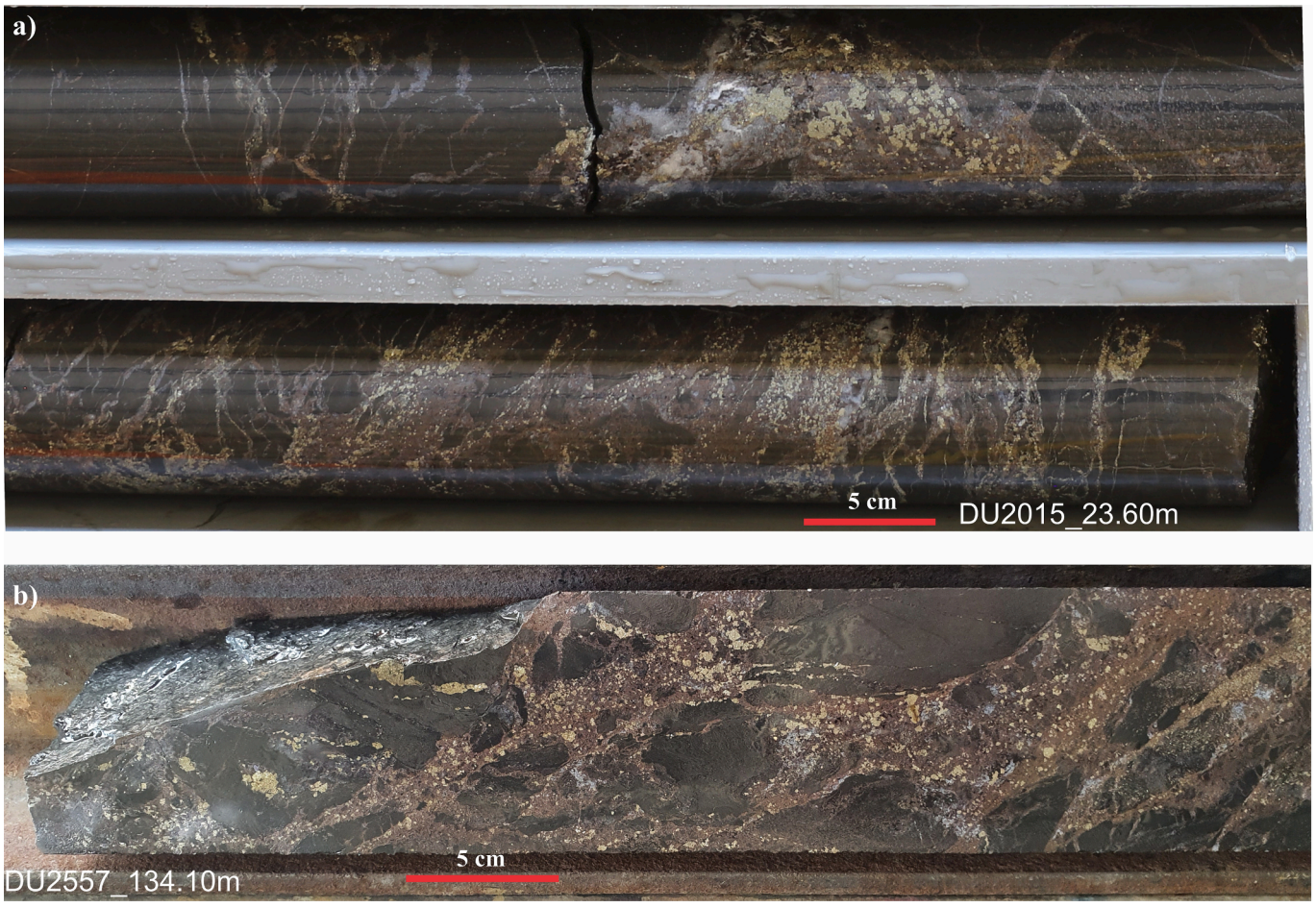

Fig. 15. Hand specimen representation of a durchbewegung structure. At the interface of a sulphide layer and slate, the slate fractures with the cracks infilled with sulphides, whereas the sulphides can deform through ductile means and flow through the rocks. Slate clasts are incorporated into the sulphide layer and through a process of kneading, milling and rolling are rounded. The inferred temperature range falls within 350–500°, which is the temperature at which most sulphides deform in a ductile manner except for pyrite. Here, this is illustrated by the abundance of pyrite within the sulphide layers and sphalerite infilling the cracks. Furthermore, some pyrite grains in (a) are sub-rounded. a) Grid reference: 3C. b) Grid reference: 4E.

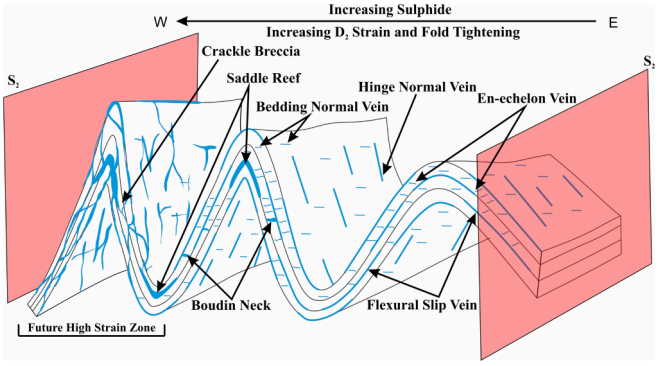

Fig. 16. Cartoon sketch of Phase 1 mineralisation. Progressive tightening of folds resulted in secondary space accommodating quartz-carbonate veins (blue lines and polygons), progressively steepening parallel to steep, W-dipping S_2 planes. Where fold interlimb angles are tight, veins create interconnected networks that are now sub-parallel to S_2, and a crackle breccia developed where wall-rock to sulphide ratios are lower. Zones of crackle breccia and closely spaced, interconnected veins created a favourable heterogeneous rock mass for strain partitioning during D_3 and D_4. Notably, these zones are sites for future high strain zone development.

veins, sulphide deposition and deformation were coeval as indicated by progressive migration of veins and sulphides into dilational sites where folding has intensified (i.e., fold hinge separation and boudinage along fold limbs; Davis, 2017). Away from the ore body, layer-parallel veins (flexural slip veins) are spaced (>10 cm), thinner and relatively evenly distributed, but the sulphide concentration is negligible. Closer to the ore body the spacing between quartz-carbonate veins becomes increasingly smaller, veins are thicker, and the concentration of sulphides increases. Folds are close to isoclinal with hinge separation (saddle reef) and boudinage in fold limbs (e.g., Fig. 14a).

Increasing D_2 strain resulted in progressive fold tightening and cumulative fold accommodation veins that were rotated into parallelism with S_2. Zones of tight to isoclinal folds with associated, coalesced sulphide replaced quartz-carbonate veins resemble a crackle breccia. We infer that this zone of incipient brecciation produced a heterogenous rock mass that was favourable for S_3 intensification during D_3, which in turn favoured early D_4 reactivation as low-angle thrusts and initial dilation for intense brecciation during prevailing D_4 shearing. In other areas, like the North Mine, fold amplification and steepening of F_2 fold limbs resulted in vein rotation into parallelism with S_2 and form the precursor to planar ore during D_4.

6.3. *Intervening phase*

Following D_2 is an inferred period of orogenic collapse, whereby, the stress exerted by an overthickened orogen exceeds the compressive stress due to shortening and in the Mount Isa Inlier this resulted in sub-vertical principal stress with a suggested top-to-the-E sense of shear (e.g., Xu, 1996; Bell and Hickey, 1998; Murphy, 2004). Notably, this involved a switch from a sub-horizontal principal stress direction and associated sub-vertical fabric development (i.e., S_2 and upright F_2 folds) to a sub-vertical principal stress direction and associated sub-horizontal fabric development (S_3).

The effects of D_3 are subtle and within the Dugald River deposit generally occur as a spaced crenulation cleavage. In the South Mine, the heterogenous rock mass resulting from F_2 fold tightening and crackle breccia formation provided favourable sites for zones of S_3 intensification (Fig. 17a). The zones of S_3 intensification locally rotated steeply dipping S_0 and S_2 orientations to lower angle, ~west dipping orientations (also Xu, 1996). In addition, this would have rotated F_2 to more recumbent orientations with sub-horizontal axial planes, however, this was not observed during underground mapping and drillcore analysis

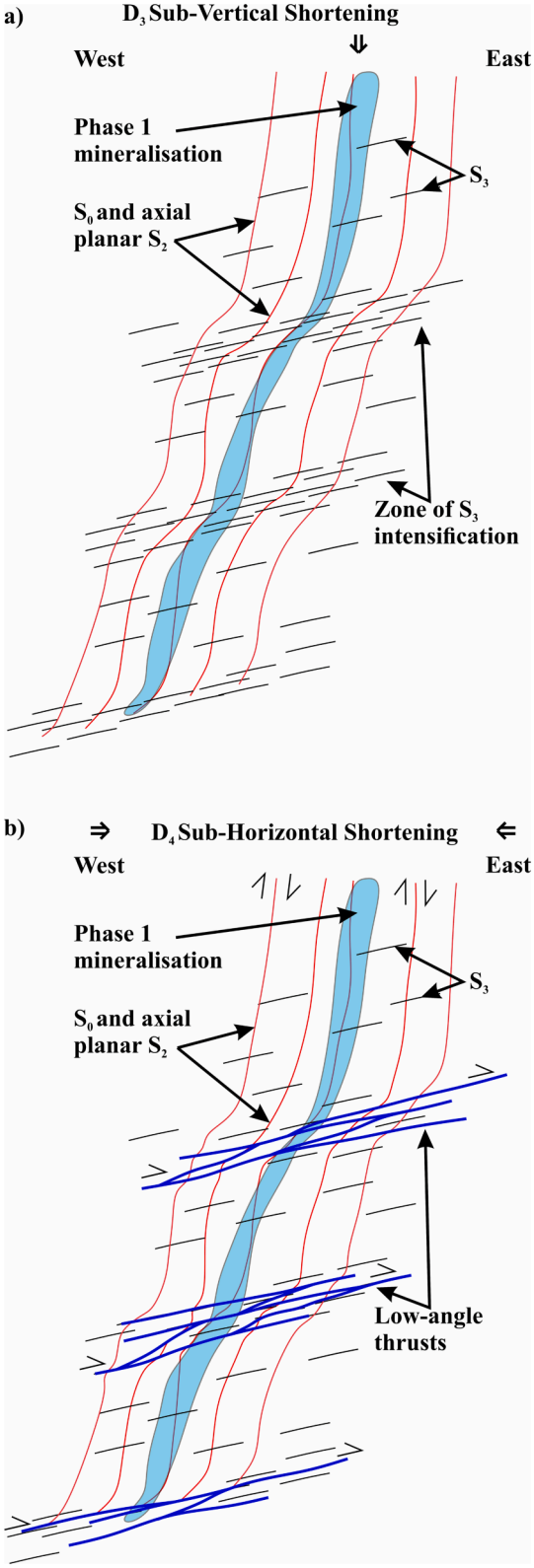

Fig. 17. A) During a period of inferred orogenic collapse, the D_3 principal stress direction was sub-vertical, which produced sub-horizontal S_3 planes. In the South Mine, zones of S_3 intensification locally rotated Phase 1 mineralisation (in blue) and steep S_0 and S_2 to lower angle, ~ west dips. b) During D_4, with the resumption of E-W directed compressive stress, the cleavage planes within the zones of S_3 intensification were reactivated and linked to form low-angle thrusts that ramp to form low-angle lenses. Low-angle thrusts are common in grid reference 4D.

but was described by Xu (1996) away from the deposit on the surface.

6.4. Phase 2 mineralisation

Phase 2 mineralisation is inferred to have occurred during retrograde metamorphism, during the waning stages of the Isan Orogeny. Thus, this involved a transition from ductile to brittle-ductile deformation (e.g., O'Dea et al., 1997). Following the period of orogenic collapse, the continuation of bulk E-W sub-horizontal shortening resulted in the reactivation of zones of intensified S_3 in the South Mine as low-angle thrusts with a top-to-the-NE sense of shear (Fig. 17). Opposing shear along stacked thrusts created zones of contraction and extension, i.e., areas of high and low mean rock stress, respectively, promoting remobilisation of sulphides. Additionally, synthetic shear along steeper S_0 and S_2 created additional zones of dilation with subsequent remobilisation of sulphides into the zones.

The asymmetry of sigmoidal lenses in the S-C' fabric is consistent with a top-to-the-NE sense of shear. Notably, given that D_4 was ~E-W directed (O'Dea et al., 1997), steep W-dipping S_0 and S_2 planes were in favourable orientations for synthetic, dextral shear and S_3 planes to accommodate dip-slip movements. Furthermore, increasing strain during D_4 is marked by a progression from coaxial to non-coaxial strain.

Fabric formation during early D_4 involved a coaxial strain history. The effects are best preserved in the North Mine where further tightening of F_2 resulted in textures that are similar to Phase 1 mineralisation (i.e., attenuation of fold limbs and migration of sulphides into extensional sites. The steep fabric elements (S_0, isoclinal F_2 folds, and an axial planar S_2 fabric), combined with progressive tightening of folds into parallelism with S_2, resulted in the development of a transposition fabric and eventually high strain zones that wrapped around low strain zones with preserved F_2 folds (Figs. 18, 19b). In the South Mine, the effects of coaxial strain have been preserved in zones away from low-angle thrusts where opposing shear along steep, W-dipping S_0 and S_2 versus top-to-the-NE movement along the thrusts resulted in dilation and areas of low mean rock stress.

With the exhumation of the deposit and a transition from ductile to brittle-ductile deformation, the P-T conditions were within the range for ductile deformation of sulphides versus brittle deformation of the slate. The transition from ductile to brittle-ductile deformation was marked by a switch from coaxial to non-coaxial deformation largely due to the thickened sulphide horizon in the South Mine. The sulphides could deform in a ductile manner versus the host slate that had to accommodate the strain in a brittle manner. Riedel shears developed within the slates and in an en-echelon manner (see Creus, 2022). The first Riedel shears to develop are R-shears with R'-shears developed within overlap zones between R-shears – an effect that is prominent in the South Mine. Thus, opposing shear along numerous Riedel shears and low-angle thrusts resulted in the widespread development of contractional and extensional sites within the South Mine promoting mechanical remobilisation of sulphides and durchbewegung structures to develop. With increasing strain, P-shears developed and as the shear segments grew, they interconnected with R-shear segments to develop throughgoing Y-shears eventually forming an anastomosing shear zone.

Shear zones are effective channel ways for transporting fluids. The shear zone is largely developed within impermeable slates and it is plausible that the Dugald River Shear Zone transported fluids from depth and given that the South Mine represents a bulk area of low mean rock stress, ingress of fluids into this zone may have occurred (Fig. 20). Thus, while numerous fracture planes developed within the host rock during which opposing and converging shear created zones of dilation and contraction, respectively, the inferred fluid injection coupled with mechanical remobilisation will have significantly enriched mineralisation.

Phase 2 mineralisation is inferred to have been episodic and probably long-lived given helical inclusion trails and polycrystalline growth of quartz around rounded, vein quartz. Micro-textural and hand

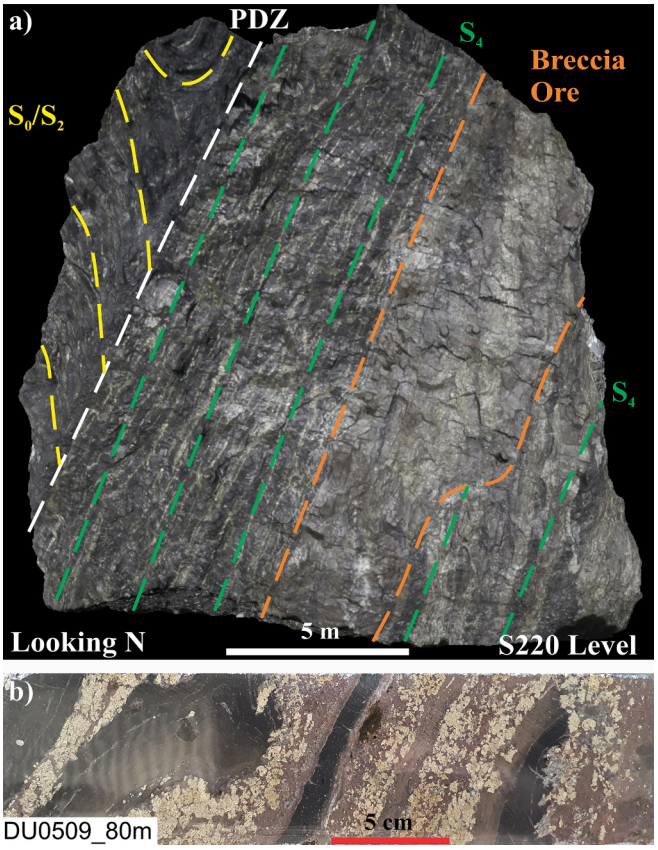

Fig. 18. A) SfM-MVS capture of S220_OD430_S1 level (grid reference 4C). In the South Mine the planar ore is preserved where the shear zone is steep and commonly disrupted by metre-scale lenses of breccia ore. The principal displacement zone (PDZ) shown on the capture is relatively thin compared to other examples (e.g., Fig. 8–10). The shear zone truncates a low strain domain to the west, which preserves folded S_0, as well as sulphide replaced flexural slip veins that were rotated into parallelism with S_2 as folds tightened. b) Hand specimen example of transposition of folded slate and sulphide. In addition, strength contrasts in the sulphides has resulted in banding of sphalerite and pyrite. Sphalerite at the inferred P-T conditions was susceptible to plastic flow hence the finer-grained crystals compared pyrite that annealed to form larger crystals.

specimen investigations indicate that during this period sphalerite was the dominant sulphide species and formed the matrix of high-grade breccia ores. Wall rock clasts include polycrystalline quartz with sulphides (pyrite, sphalerite, galena and pyrrhotite) and are commonly folded, which includes Phase 1 mineralisation indicated by course-grained sulphides in the matrix (Fig. 13e).

6.4.1. North Mine

The North Mine is characterised by a steep fabric disrupted by F_2 folds (Fig. 19). Here flattening strain dominates, which progressively tightened F_2 folds and rotated veins into parallelism with S_2 (Fig. 14b), which given the co-planar D_2 and D_4 are at a high angle to the bulk sub-horizontal E-W shortening of D_4. In underground development, a significant strain gradient can be observed when moving west from the limestone towards the shear zone. Near the limestone contact within the slates, S_0 is distinguishable from axial planar S_2 to F_2 folds. Within metres of the shear zone, F_2 folds are observed to be isoclinal and contained within the transposed fabric, creating high and low strain domains.

The North Mine has a general lack of breccia ore. An explanation for this is that the North Mine lacks a major structural control for breccia ore to have developed, namely, the low-angle thrusts. Thus, zones of

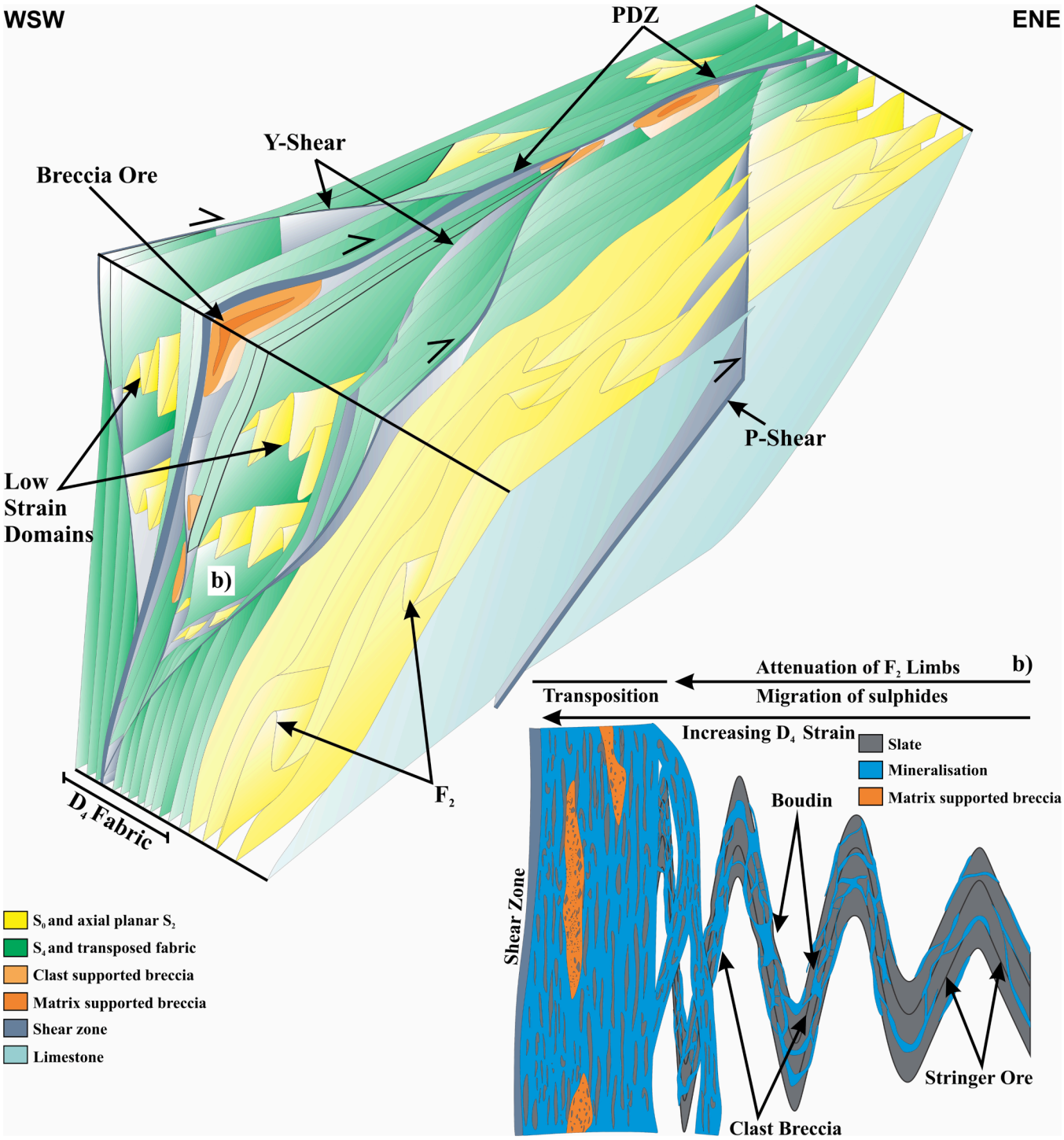

Fig. 19. Cartoon sketch of the North Mine. In the North Mine, steeper S_0 and axial planar S_2 with upright folds, which have arrays of sub-parallel veins were transposed during D_4 (b). Transposition has resulted in the development of high and low strain domains. High strain domains have preferentially developed in the sulphide horizon and are marked by the development of a transposition fabric, S_4, with alternating slate and sulphide veins (Fig. 13d, Fig. 18b). Rootless F_2 folds occur within high strain domains and low strain domains are marked by preserved synform-antiform pairs of F_2. Dextral shearing during D_4 resulted in the development of the anastomosing Dugald River Shear Zone. In the North Mine, planar ore is the dominant ore texture and breccia ore is developed in undulations in the shear zone. b) The progressive tightening of folds resulted in the development of a transposition fabric with increasing strain. Attenuation of fold limbs and boudinage resulted in interlinking of veins. The ratio of wall rock to veins and the orientation of the veins are used to label the ore textures (i.e., stringer and planar ore, clast breccia) with overlap between the named textures.

contraction and extension were lacking, and the strain was accommodated by progressive fold tightening leading to transposition. The planar ore (stringer and banded ore textures) represents transposed Phase 1 mineralisation and the wall rock to sulphide ratio is too low for durchbewegung structures to develop. Furthermore, given the steep fabric, the development of dilational jogs is limited to undulations in the shear zone and the South Mine acted as a sink for ingress fluid ingress along the shear zone.

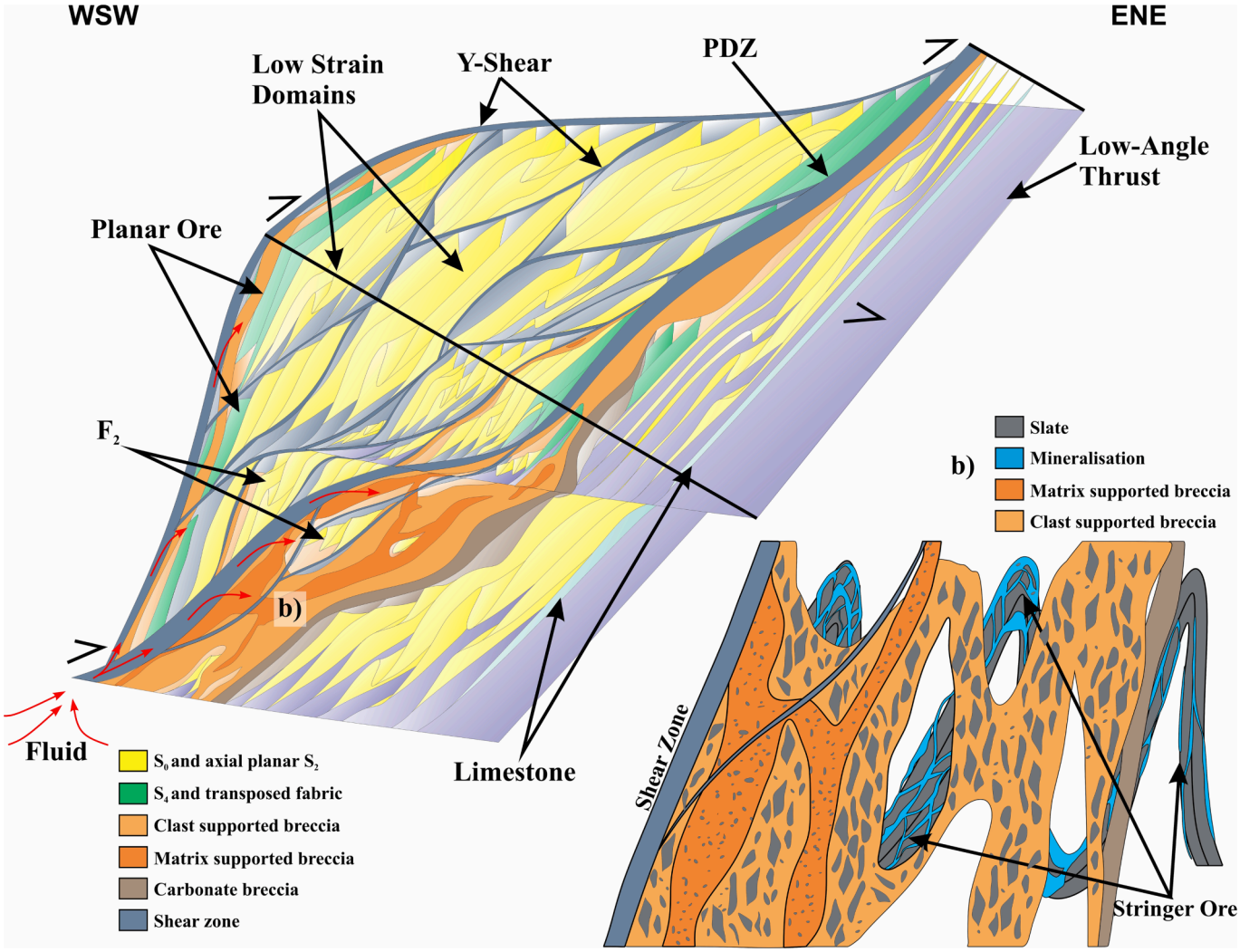

Fig. 20. Cartoon sketch of the South Mine. The South Mine is marked by a thicker and higher-grade ore zone, which is dominated by breccia type ore. The dextral step-over in the shear zone resulted in the formation of a dilational jog and a favourable geometry for durchbewegung structures to develop. Early D_4 involved the reactivation of moderate SW-dipping S_3 to form low-angle thrusts with a top-to-the-NE sense of shear. Where the low-angle thrusts intersected steep, W-dipping S_0 and S_2, opposing shear directions resulted in dilation. In areas where low-angle thrusts do not occur, increasing strain during D_4 resulted in transposition and development of planar ore (shown in green). With the onset of shear development, the shear zone acted as a channel way for Zn-rich fluid (red arrows) with the step-over acting as a preferential depositional site. b) With an increase in the sulphide to wall-rock ratio, mechanical shearing (durchbewegung) resulted in enrichment of sulphides and a significant increase in the Zn-grade.

6.4.1.1. South Mine. The South Mine is dominated by breccia ore (Fig. 13a). While planar ore is observed in the South Mine, this type of ore texture is limited to steep parts of the shear zone where the effects of S_3 reactivation are limited and has been largely disrupted by durchbewegung textures responsible for the breccia ore. The initial stages of Phase 2 mineralisation in the South Mine follow those of the North Mine, with the exception that along intersection zones of opposing low-angle thrusts to steep, W-dipping fabric, areas of low mean rock stress developed with associated migration of sulphides.

With the onset of shearing, the combination of low-angle thrusts, flattened S_0 and S_2 resulted in a favourable geometry for a step-over to develop in the shear zone. Thus, fluid migrating up the channel way created by the shear zone, which is enveloped by impermeable lithologies, eventually reached the dilational zone created by the step-over. A high sulphide to wall rock ratio resulted and given the ductile nature of the sulphides versus the more brittle nature of the host rocks, durchbewegung structures developed. Notably, this step-over represents a significant area of low mean rock stress over the rest of the deposit, and it is inferred that most of the Zn-rich fluid migrated here via mixed-state solution.

7. Conclusion

- The Dugald River deposit has been subjected to several deformation events during the Isan Orogeny. Co-planar progressive deformation during D_2 and D_4 provided favourable extensional sites for the mineralising fluid to deposit sulphides including sphalerite during two phases of mineralisation, namely, Phase 1 and Phase 2 mineralisation.
- Phase 1 mineralisation is associated with progressive tightening of folds during a regionally extensive, ductile deformation event (D_2). Flexural slip, hinge-normal and bedding-normal quartz-carbonate veins were progressively rotated into parallelism with the pervasive S_2 fabric and replaced by sulphides. This phase was sub-economic.
- An inferred period of orogenic collapse, D_3, provided an important structural control for high-grade mineralisation during D_4. Zones of S_3 intensification were heterogeneously developed and prominent in the South Mine. Reactivation of S_3 planes during D_4 produced low-angle thrusts along which opposing shear resulted in contractional and extensional sites, promoting sulphide migration and thickening of the sulphide horizon in the South Mine.

- Early Phase 2 mineralisation was deposited during D_4 ductile shearing as a result of progressive fold tightening which produced a transposed fabric of sulphides and slate (planar ore). The North Mine lacks the structural control of low-angle thrusts, however, the concentration of the sulphides due to transposition resulted in economic grade mineralisation.
- With exhumation of the deposit and a transition to D_4 brittle-ductile shearing, there was a significant enrichment of the deposit through mixed-state solution, particularly in the South Mine. Zn-enriched fluid exploited channel ways developed by the shearing and the step-over created in the shear zone by low-angle thrusts. Mechanical remobilisation migrated sulphides that deformed in a ductile manner from areas of high to low mean rock stress, infilling cracks in the competent wall rock fragments that were progressively kneaded, milled and rolled into smaller and rounder fragments.

Declaration of Competing Interest

The authors declare that they have no known competing financial interests or personal relationships that could have appeared to influence the work reported in this paper.

Data availability

The authors do not have permission to share data.

Acknowledgements

The authors acknowledge MMG Dugald River mine for funding and support. The corresponding author acknowledges James Cook University for providing a Ph.D. scholarship. Agisoft are acknowledged for providing an educational license for Metashape. Seequent, Paradigm and Mira Geoscience are thanked for providing academic licences for Leapfrog Geo, SKUA-GoCAD and GoCAD Mining Suite 3D modelling software, respectively. The mining technical services department at Dugald River mine are thanked for their support during this study. The reviewers are thanked for their comments and contributions to the improving the quality of the manuscript.

References

Abu Sharib, A.S.A.A., Bell, T.H., 2011. Radical changes in bulk shortening directions during orogenesis; significance for progressive development of regional folds and thrusts. Precambr. Res. 188 (1–4), 1–20. https://doi.org/10.1016/j.precamres.2011.03.008.

Abu Sharib, A.S.A.A., Sanislav, I.V., 2013. Polymetamorphism accompanied switching in horizontal shortening during Isan Orogeny; example from the Eastern fold belt, Mount Isa Inlier, Australia. Tectonophysics 587, 146–167. https://doi.org/10.1016/j.tecto.2012.06.051.

Aerden, D.G.A.M., 1991. Foliation-boudinage control on the formation of the Rosebery Pb-Zn orebody, Tasmania. J. Struct. Geol. 13 (7), 759–775. https://doi.org/10.1016/0191-8141(91)90002-Z.

Anovitz, L.M., Essene, E.J., 1987. Phase equilibria in the system $CaCO_3$-$MgCO_3$-$FeCO_3$. J. Petrol. 28 (2), 389–415. https://doi.org/10.1093/petrology/28.2.389.

Arslan, A., Passchier, C.W., Koehn, D., 2008. Foliation boudinage. J. Struct. Geol. 30 (3), 291–309. https://doi.org/10.1016/j.jsg.2007.11.004.

Arslan, A., Koehn, D., Passchier, C.W., Sachau, T., 2012. The transition from single layer to foliation boudinage; a dynamic modelling approach. J. Struct. Geol. 42, 118–126. https://doi.org/10.1016/j.jsg.2012.06.005.

ASUD (2021). Australian Stratigraphic Units Database.

Bell, T.H., 1983. Thrusting and duplex formation at Mount Isa, Queensland, Australia. Nature (London) 304 (5926), 493–497. https://doi.org/10.1038/304493a0.

Bell, T.H., Hickey, K.A., 1998. Multiple deformations with successive subvertical and subhorizontal axial planes in the Mount Isa region; their impact on geometric development and significance for mineralization and exploration. Econ. Geol. 93 (8), 1369–1389. https://doi.org/10.2113/gsecongeo.93.8.1369.

Bell, T.H., Reinhardt, J.W., Hammond, R.L., 1992. Multiple foliation development during thrusting and synchronous formation of vertical shear zones. J. Struct. Geol. 14 (7), 791–805. https://doi.org/10.1016/0191-8141(92)90041-T.

Betts, P.G., Giles, D., Mark, G., Lister, G.S., Goleby, B.R., Ailleres, L., 2006. Synthesis of the Proterozoic evolution of the Mt Isa Inlier. Aust. J. Earth Sci. 53 (1), 187–211. https://doi.org/10.1080/08120090500434625.

Betts, P.G., Giles, D., Schaefer, B.F., 2008. Comparing 1800–1600 Ma accretionary and basin processes in Australia and Laurentia; possible geographic connections in Columbia. Precambr. Res. 166 (1–4), 81–92. https://doi.org/10.1016/j.precamres.2007.03.007.

Bierlein, F.P., Maas, R., Woodhead, J., 2011. Pre-1.8 Ga tectono-magmatic evolution of the Kalkadoon-Leichhardt Belt; implications for the crustal architecture and metallogeny of the Mount Isa Inlier, northwest Queensland, Australia. Aust. J. Earth Sci. 58 (8), 887–915. https://doi.org/10.1080/08120099.2011.571286.

Blake, D.H., 1987. Geology of the Mount Isa Inlier and environs, Queensland and Northern Territory. BMR Bull. 225, 83.

Blake, D.H., Stewart, A.J. (1992). Stratigraphic and tectonic framework, Mount Isa Inlier. Detailed Studies of the Mount Isa Inlier. Australian Geological Survey Organisation, 1–11.

Bodon, S.B., 1998. Paragenetic relationships and their implications for ore genesis at the Cannington Ag-Pb-Zn deposit, Mount Isa Inlier, Queensland, Australia. Econ. Geol. 93 (8), 1463–1488. https://doi.org/10.2113/gsecongeo.93.8.1463.

Bodon, S.B., 2002. Geodynamic Evolution and Genesis of the Cannington Broken Hill-type Ag-Pb-Zn deposit, Mount lsa Inner, Queensland. University of Tasmania, p. 443p. Unpublished PhD thesis.

Broadbent, G.C., Myers, R.E., Wright, J.V., 1998. Geology and origin of shale-hosted Zn-Pb-Ag mineralization at the Century Deposit, Northwest Queensland, Australia. Econ. Geol. 93 (8), 1264–1294. https://doi.org/10.2113/gsecongeo.93.8.1264.

Cave, B., Lilly, R., Barovich, K., 2020. Textural and geochemical analysis of chalcopyrite, galena and sphalerite across the Mount Isa Cu to Pb-Zn transition: implications for a zoned Cu-Pb-Zn system. Ore Geol. Rev. 124, 103647. https://doi.org/10.1016/j.oregeorev.2020.103647.

Chapman, L.H., 2004. Geology and mineralization styles of the George Fisher Zn-Pb-Ag deposit, Mount Isa, Australia. Econ. Geol. 99 (2), 233–255. https://doi.org/10.2113/gsecongeo.99.2.233.

Chapman, 1998. P.J.Evolution of pyroxene-pyroxenoid-garnet alteration at the Cannington Ag-Pb-Zn deposit, Cloncurry District, Queensland, Australia. Econ. Geol. 93 (8), 1390–1405. https://doi.org/10.2113/gsecongeo.93.8.1390.

Connor, A.G., Johnson, I.R., Muir, M.D., 1982. The Dugald River zinc-lead deposit, northwest Queensland, Australia. Proc. Australas. Inst. Min. Metall. 283, 1–19.

Connors, K.A., Proffett, J.M., Lister, GS., Scott, R. J., Oliver, N.H.S., Young, D.J. (1992). Geology of the Mount Novit Ranges, southwest of Mount Isa mine, in: Stewart, A.J. & Blake, D.H. (Eds.), Detailed Studies of the Mount Isa Inlier. Bureau of Mineral Resources, Geology and Geophysics, pp. 137–160.

Connors, K.A., Page, R.W., 1995. Relationships between magmatism, metamorphism and deformation in the western Mount Isa Inlier, Australia. Precambr. Res. 71 (1–4), 131–153. https://doi.org/10.1016/0301-9268(94)00059-Z.

Cook, N.J., Halls, C., Boyle, A.P., 1993. Deformation and metamorphism of massive sulphides at Sulitjelma, Norway. Mineral. Mag. 57 (1(386)), 67–81. https://doi.org/10.1180/minmag.1993.057.386.07.

Craig, J.R., Vokes, F.M., Solberg, T.N., 1998. Pyrite; physical and chemical textures. Miner. Deposita 34 (1), 82–101. https://doi.org/10.1007/s001260050187.

Creus, P.K., 2022. 3D structural controls of the shear zone hosted Dugald River zinc-lead-silver deposit, Mount Isa Inlier, Australia. James Cook University. Ph.D. thesis.

Creus, P.K., Sanislav, I.V., Dirks, P.H.G.M., 2021. Application of SfM-MVS for mining geology: Capture set-up and automated processing using the Dugald River Zn-Pb-Ag mine as a case study. Eng. Geol. 293, 106314. https://doi.org/10.1016/j.enggeo.2021.106314.

Davidson, G.J., Davis, B.K., Garner, A., 2002. Structural and geochemical constraints on the emplacement of the Monakoff Oxide Cu-Au(-Co-U-REE-Ag-Zn-Pb) deposit, Mt Isa Inlier, Australia. In: Porter, T.M. (Ed.), Hydrothermal Iron Oxide Copper-Gold & Related Deposits: A Global Perspective. PGC Publishing, Adelaide, pp. 49–75.

Davis, T.P., 2004. Mine-scale structural controls on the Mount Isa Zn-Pb-Ag and Cu Orebodies. Econ. Geol. 99 (3), 543–559. https://doi.org/10.2113/99.3.543.

Davis, G.H., Bump, A.P., Garcia, P.E., Ahlgren, S.G., 2000. Conjugate Riedel deformation band shear zones. J. Struct. Geol. 22 (2), 169–190. https://doi.org/10.1016/S0191-8141(99)00140-6.

Davis, B.K. (2017). Dugald River - Orebody Knowledge Study (DROKS). Unpublished report by Orefind.

Derrick, G.M., Wilson, I.H., Hill, R., 1977. Revision of stratigraphic nomenclature in the Precambrian of northwestern Queensland. VII: Mount Albert Group. Queensl. Gov. Min. J. 77, 113–116.

Dirks, P.G.H.M., Charlesworth, E.G., Munyai, M.R., 2009. Cratonic extension and Archaean gold mineralisation in the Sheba-Fairview mine, Barberton Greenstone Belt, South Africa. S. Afr. J. Geol. 112 (3–4), 291–316. https://doi.org/10.2113/gssajg.112.3-4.291.

Dirks, P.H.G.M., Charlesworth, E.G., Munyai, M.R., Wormald, R., 2013. Stress analysis, post-orogenic extension and 3.01 Ga gold mineralisation in the Barberton greenstone belt, South Africa. Precambr. Res. 226, 157–184. https://doi.org/10.1016/j.precamres.2012.12.007.

Dixon, G., Davidson, G.J., 1996. Stable isotope evidence for thermochemical sulfate reduction in the Dugald River (Australia) strata-bound shale-hosted zinc-lead deposit. Chem. Geol. 129 (3–4), 227–246. https://doi.org/10.1016/0009-2541(95)00177-8.

Feltrin, L., McLellan, J.G., Oliver, N.H.S., 2009. Modelling the giant, Zn-Pb-Ag century deposit, Queensland, Australia. Comput. Geosci. 35 (1), 108–133. https://doi.org/10.1016/j.cageo.2007.09.002.

Finlow-Bates, T., Stumpfl, E.F., 1979. The copper and lead-zinc-silver orebodies of Mt Isa Mines, Queensland: products of one hydrothermal system. Ann. la Soc. Geol. Belgique 102, 497–517.

Foster, D., Austin, J., 2008. The 1800–1610Ma stratigraphic and magmatic history of the Eastern Succession, Mount Isa Inlier, and correlations with adjacent

Paleoproterozoic terranes. Precambr. Res. 163 (1–2), 7–30. https://doi.org/10.1016/j.precamres.2007.08.010.
Foster, D.R.W., Rubenach, M.J., 2006. Isograd pattern and regional low-pressure, high-temperature metamorphism of pelitic, mafic and calc-silicate rocks along an east-west section through the Mt Isa Inlier. Aust. J. Earth Sci. 53 (1), 167–186. https://doi.org/10.1080/08120090500434617.
George, K.-L. (2011). Mineralisation processes at the Dugald RIver Pb-Zn-Ag deposit, Mount Isa Eastern Inlier, NW Queensland. Unpublished honours thesis. James Cook University of North Queensland. 143pp.
Gibson, G.M., Hitchman, A.P., 2005. Project I1 Final Report. Geoscience Australia, Canberra.
Gibson, G.M., Rubenach, M.J., Neumann, N.L., Southgate, P.N., Hutton, L.J., 2008. Syn- and post-extensional tectonic activity in the Palaeoproterozoic sequences of Broken Hill and Mount Isa and its bearing on reconstructions of Rodinia. Precambr. Res. 166 (1–4), 350–369. https://doi.org/10.1016/j.precamres.2007.05.005.
Gibson, G.M., Henson, P.A., Neumann, N.L., Southgate, P.N., Hutton, L.J., 2012. Paleoproterozoic-earliest Mesoproterozoic basin evolution in the Mount Isa region, northern Australia and implications for reconstructions of the Nuna and Rodinia supercontinents. Episodes 35 (1), 131–141.
Gibson, G.M., Meixner, A.J., Withnall, I.W., Korsch, R.J., Hutton, L.J., Jones, L.E.A., Holzschuh, J., Costelloe, R.D., Henson, P.A., Saygin, E., 2016. Basin architecture and evolution in the Mount Isa mineral province, northern Australia; constraints from deep seismic reflection profiling and implications for ore genesis. Ore Geol. Rev. 76, 414–441.
Giles, D., Betts, P.G., Ailleres, L., Hulscher, B., Hough, M., Lister, G.S., 2006. Evolution of the Isan Orogeny at the southeastern margin of the Mt Isa Inlier. Aust. J. Earth Sci. 53 (1), 91–108. https://doi.org/10.1080/08120090500432470.
Gulson, B.L., Perkins, W.G., Mizon, K.J., 1983. Lead isotope studies bearing on the genesis of copper orebodies at Mount Isa, Queensland. Econ. Geol. 78 (7), 1466–1504. https://doi.org/10.2113/gsecongeo.78.7.1466.
Hobbs, B.E., 1987. Principles involved in mobilization and remobilization. Ore Geol. Rev. 2 (1–3), 37–45. https://doi.org/10.1016/0169-1368(87)90022-9.
Huston, D.L., Stevens, B., Southgate, P.N., Muhling, P., Wyborn, L., 2006. Australian Zn-Pb-Ag ore-forming systems; a review and analysis. Econ. Geol. 101 (6), 1117–1157. https://doi.org/10.2113/gsecongeo.101.6.1117.
Jackson, M.J., Scott, D.L., Rawlings, D.J., 2000. Stratigraphic framework for the Leichhardt and Calvert superbasins; review and correlations of the pre-1700 Ma successions between Mt Isa and McArthur River. Aust. J. Earth Sci. 47 (3), 381–403. https://doi.org/10.1046/j.1440-0952.2000.00789.x.
Klemd, R., Maiden, K.J., Okrusch, M., 1987. The Matchless copper deposit, South West Africa/Namibia; a deformed and metamorphosed massive sulfide deposit. Econ. Geol. 82 (3), 587–599. https://doi.org/10.2113/gsecongeo.82.3.587.
Large, R.R., Bull, S.W., McGoldrick, P.J., Walters, S., Derrick, G.M., Carr, G.R., 2005. Stratiform and stratabound Zn-Pb-Ag deposits in Proterozoic sedimentary basins, northern Australia. Econ. Geol. 100th Anniv. 931–963.
Le, T.X., Dirks, P.H.G.M., Sanislav, I.V., Huizenga, J.M., Cocker, H.A., Manestar, G.N., 2021a. Geochronological constraints on the geological history and gold mineralization in the Tick Hill region, Mt Isa Inlier. Precambr. Res. 366, 106422.
Le, T.X., Dirks, P.H.G., Sanislav, I.V., Huizenga, J.M., Cocker, H.A., Manestar, G.N., 2021b. Geological setting and mineralization characteristics of the Tick Hill Gold Deposit, Mount Isa Inlier, Queensland, Australia. Ore Geol. Rev. 137, 104288. https://doi.org/10.1016/j.oregeorev.2021.104288.
Loosveld, R., Schreurs, G., 1987. Discovery of thrust klippen, northwest of Mary Kathleen, Mt. Isa Inlier, Australia. Aust. J. Earth Sci. 34 (3), 387–402. https://doi.org/10.1080/08120098708729419.
Maiden, K.J., Chimimba, L.R., Smalley, T.J., 1986. Cuspate ore-wall rock interfaces, piercement structures and the localization of some sulfide ores in deformed sulfide deposits. Econ. Geol. 81 (6), 1464–1472. https://doi.org/10.2113/gsecongeo.81.6.1464.
Marshall, B., Gilligan, L.B., 1987. An introduction to remobilization; information from ore-body geometry and experimental considerations. Ore Geol. Rev. 2 (1–3), 87–131. https://doi.org/10.1016/0169-1368(87)90025-4.
Marshall, B., Gilligan, L.B., 1989. Durchbewegung structure, piercement cusps, and piercement veins in massive sulfide deposits; formation and interpretation. Econ. Geol. 84 (8), 2311–2319. https://doi.org/10.2113/gsecongeo.84.8.2311.
Marshall, B., Gilligan, L.B., 1993. Remobilization, syn-tectonic processes and massive sulphide deposits. Ore Geol. Rev. 8 (1–2), 39–64. https://doi.org/10.1016/0169-1368(93)90027-V.
Marshall, B., Vokes, F., Larocque, A., 2000. Regional metamorphic remobilization: upgrading and formation of ore deposits. Rev. Econ. Geol. 11, 19–38.
McGoldrick, P.J., Keays, R.R., 1990. Mount Isa copper and lead-zinc-silver ores; coincidence or cogenesis? Econ. Geol. 85 (3), 641–650. https://doi.org/10.2113/gsecongeo.85.3.641.
McQueen, K.G., 1987. Deformation and remobilization in some Western Australian nickel ores. Ore Geol. Rev. 2 (1–3), 269–286. https://doi.org/10.1016/0169-1368(87)90032-1.
MMG (2021). MMG Limited mineral resources and ore reserves statement as at 30 June 2021. 220pp.
Mueller, A.G., 2020. Structural setting of Fimiston- and Oroya-style pyrite-telluride-gold lodes, Paringa South Mine, Golden Mile, Kalgoorlie; 1. Shear zone systems, porphyry dykes and deposit-scale alteration zones. Miner. Deposita 55 (4), 665–695. https://doi.org/10.1007/s00126-017-0747-3.
Murphy, T.E. (2004). Structural and stratigraphic controls on mineralization at the George Fisher Zn-Pb-Ag Deposit, Northwest Queensland, Australia. Unpublished PhD thesis. James Cook University. 443p.
Naylor, M.A., Mandl, G., Sijpesteijn, C.H.K., 1986. Fault geometries in basement-induced wrench faulting under different initial stress states. J. Struct. Geol. 8 (7), 737–752. https://doi.org/10.1016/0191-8141(86)90022-2.
Neumann, N.L., Gibson, G.M., Southgate, P.N., 2009. New SHRIMP age constraints on the timing and duration of magmatism and sedimentation in the Mary Kathleen fold belt, Mt Isa Inlier, Australia. Austral. J. Earth Sci. 56 (7), 965–983. https://doi.org/10.1080/08120090903005410.
Newbery, S.P., Carswell, J.T., Allnutt, S.L. & Mutton, A.J., 1993. The Dugald River zinc-lead-silver deposit; an example of a tectonised Proterozoic stratabound sulphide deposit, in: International Symposium - World Zinc '93. Hobart, pp. 7–21.
Nortje, G.S., Oliver, N.H.S., Blenkinsop, T.G., Keys, D.L., McLellan, J.G., Oxenburgh, S., 2011. New faults v. fault reactivation; implications for fault cohesion, fluid flow and copper mineralization, Mount Gordon fault zone, Mount Isa District, Australia. Geochem. Soc. Spec. Publ. 359 (1), 287–311. https://doi.org/10.1144/SP359.16.
O'Dea, M.G., Lister, G.S., Maccready, T., Betts, P.G., Oliver, N.H.S., Pound, K.S., Huang, W., Valenta, R.K., Oliver, N.H.S., Valenta, R.K., 1997. Geodynamic evolution of the Proterozoic Mount Isa terrain. Geol. Soc. Special Publ. 121 (1), 99–122. https://doi.org/10.1144/GSL.SP.1997.121.01.05.
Oliver, N.H.S., Holcombe, R.J., Hill, E.J., Pearson, P.J., 1991. Tectono-metamorphic evolution of the Mary Kathleen fold belt, Northwest Queensland; a reflection of mantle plume processes? Aust. J. Earth Sci. 38 (4), 425–455. https://doi.org/10.1080/08120099108727982.
O'Rourke, A.J., Johnson, B.N.B., King, S. (2017). Century Zn-Pb-Ag, in: Pjillips, G. N. (Ed.), Australian Ore Deposist. Australian Institute of Mining and Mettalurgy, 485 - 492.
Page, R.W., 1983. Timing of superposed volcanism in the Proterozoic Mount Isa Inlier, Australia. Precambr. Res. 21 (3/4), 223–245. https://doi.org/10.1016/0301-9268(83)90042-6.
Page, R.W., Bell, T.H., 1986. Isotopic and structural responses of granite to successive deformation and metamorphism. J. Geol. 94 (3), 365–379. https://doi.org/10.1086/629035.
Page, R.W., Sun, S.S., 1998. Aspects of geochronology and crustal evolution in the Eastern Fold Belt, Mt Isa Inlier. Aust. J. Earth Sci. 45 (3), 343–361. https://doi.org/10.1080/08120099808728396.
Page, R.W., Williams, I.S., 1988. Age of the Barramundi Orogeny in northern Australia by means of ion microprobe and conventional U-Pb zircon studies. Precambr. Res. 40–41, 21–36. https://doi.org/10.1016/0301-9268(88)90059-9.
Perkins, W.G., 1997. Mount Isa lead-zinc orebodies; replacement lodes in a zoned syndeformational copper-lead-zinc system? Ore Geol. Rev. 12 (2), 61–111. https://doi.org/10.1016/S0169-1368(97)00004-8.
Perkins, W.G., Bell, T.H., 1998. Stratiform replacement lead-zinc deposits; a comparison between Mount Isa, Hilton, and McArthur River. Econ. Geol. 93 (8), 1190–1212. https://doi.org/10.2113/gsecongeo.93.8.1190.
Reinhardt, J., 1992. Low-pressure, high-temperature metamorphism in a compressional tectonic setting; the Mary Kathleen fold belt, northeastern Australia. Geol. Mag. 129 (1), 41–57. https://doi.org/10.1017/S0016756800008116.
Riedel, W. (1929). Zur mechanik geologischer Brucherscheinungen. Zentralblatt fur Mineral. Geol. und Palaontolgie 354–368.
Rieger, P., Magnall, J.M., Gleeson, S.A., Oelze, M., Wilke, F.D.H., Lilly, R., 2021. Differentiating between hydrothermal and diagenetic carbonate using rare earth element and yttrium (REE+Y) geochemistry: a case study from the Paleoproterozoic George Fisher massive sulfide Zn deposit, Mount Isa, Australia. Mineralium Deposita 57 (2), 187–206. https://doi.org/10.1007/s00126-021-01056-1.
Roache, T.J., Blenkinsop, T.G., Vearncombe, J.R., Reddy, S.M., 2004. Shear zone versus fold geometries at the Cannington Ag-Pb-Zn deposit; implications for the genesis of BHT deposits. J. Struct. Geol. 26 (6–7), 1215–1230. https://doi.org/10.1016/j.jsg.2003.11.013.
Rubenach, M.J., Lewthwaite, K.A., 2002. Metasomatic albitites and related biotite-rich schists from a low-pressure polymetamorphic terrane, Snake Creek Anticline, Mount Isa Inlier, north-eastern Australia; microstructures and P-T-d paths. J. Metam. Geol. 20 (1), 191–202. https://doi.org/10.1046/j.0263-4929.2001.00348.x.
Rubenach, M.J., Foster, D.R.W., Evins, P.M., Blake, K.L., Fanning, C.M., 2008. Age constraints on the tectonothermal evolution of the Selwyn Zone, Eastern fold belt, Mount Isa Inlier. Precambr. Res. 163 (1–2), 81–107. https://doi.org/10.1016/j.precamres.2007.08.014.
Sayab, M., 2009. Tectonic significance of structural successions preserved within low strain pods; implications for thin- to thick-skinned tectonics vs. multiple near-orthogonal folding events in the Palaeo-Mesoproterozoic Mount Isa Inlier (NE Australia). Precambr. Res. 175 (1–4), 169–186. https://doi.org/10.1016/j.precamres.2009.09.007.
Sheldon, H.A., Schaubs, P.M., Blaikie, T.N., Kunzmann, M., Poulet, T., Spinks, S.C., 2021. 3D thermal convection in the Proterozoic McArthur River Zn-Pb-Ag mineral system, northern Australia. Ore Geol. Rev. 133, 104093. https://doi.org/10.1016/j.oregeorev.2021.104093.
Smith, J.W., Burns, M.S., Croxford, N.J.W., 1978. Stable isotope studies of the origins of mineralization at Mount Isa; I. Mineralium Deposita 13 (3), 369–381. https://doi.org/10.1007/BF00206570.
Southgate, P.N., Bradshaw, B.E., Domagala, J., Jackson, M.J., Idnurm, M., Krassay, A.A., Page, R.W., Sami, T.T., Scott, D.L., Lindsay, J.F., McConachie, B.A., Tarlowski, C.Z., 2000. Chronostratigraphic basin framework for Palaeoproterozoic rocks (1730–1575 Ma) in northern Australia and implications for base-metal mineralisation. Aust. J. Earth Sci. 47 (3), 461–483. https://doi.org/10.1046/j.1440-0952.2000.00787.x.
Spampinato, G.P.T., Betts, P.G., Ailleres, L., Armit, R.J., 2015. Structural architecture of the southern Mount Isa Terrane in Queensland inferred from magnetic and gravity data. Precambr. Res. 269, 261–280. https://doi.org/10.1016/j.precamres.2015.08.017.

Spelbrink, L., George, K.-L. (2017). Dugald RIver Orebody Knowledge Study (DROKS). Unpublished internal MMG report.
Spence, J.S., Sanislav, I.V., Dirks, P.H.G.M., 2021. 1750–1710 Ma deformation along the eastern margin of the North Australia Craton. Precambr. Res. 353 https://doi.org/10.1016/j.precamres.2020.106019.
Spence, J.S., Sanislav, I.V., Dirks, P.H.G., 2022. Evidence for a 1750–1710 Ma orogenic event, the Wonga Orogeny, in the Mount Isa Inlier, Australia: Implications for the tectonic evolution of the North Australian Craton and Nuna Supercontinent. Precambr. Res. 369, 106510. https://doi.org/10.1016/j.precamres.2021.106510.
Spinks, S.M., Pearce, M.A., Liu, W., Kunzmann, M., Ryan, C.G., Moorhead, G.F., Kirkham, R., Blaikie, T., Sheldon, H.A., Schaubs, P.M., Rickard, W.D.A., 2020. Carbonate replacement as the principal ore formation process in the Proterozoic McArthur River (HYC) sediment-hosted Zn-Pb deposit, Australia. Econ. Geol. 116 (3), 693–718. https://doi.org/10.5382/econgeo.4793.
Swanson, M.T., 2006. Late Paleozoic strike-slip faults and related vein arrays of Cape Elizabeth, Maine. J. Struct. Geol. 28 (3), 456–473. https://doi.org/10.1016/j.jsg.2005.12.009.
Tchalenko, J.S., 1968. The evolution of kink-bands and the development of compression textures in sheared clays. Tectonophysics 6 (2), 159–174. https://doi.org/10.1016/0040-1951(68)90017-6.
Tomkins, A.G., 2007. Three mechanisms of ore re-mobilization during amphibolite facies metamorphism at the Montauban Zn-Pb-Au-Ag deposit. Miner. Deposita 42 (6), 627–637. https://doi.org/10.1007/s00126-007-0131-9.
Valenta, R., 1994a. Deformation of host rocks and stratiform mineralization in the Hilton Mine area, Mt Isa. Aust. J. Earth Sci. 41 (5), 429–443. https://doi.org/10.1080/08120099408728153.
Valenta, R., 1994b. Syntectonic discordant copper mineralization in the Hilton Mine Mount Isa. Econ. Geol. 89 (5), 1031–1052. https://doi.org/10.2113/gsecongeo.89.5.1031.
Vokes, F.M., 1963. Geological studies on the caledonian pyritic zinc-lead orebody at Bleikvassli, 222nd ed. Norges Geologiske UndersØkelse, Nordland, Norway.
Walters, S., Bailey, A., 1998. Geology and mineralization of the Cannington Ag-Pb-Zn deposit; an example of Broken Hill-type mineralization in the eastern succession, Mount Isa Inlier, Australia. Econ. Geol. 93 (8), 1307–1329. https://doi.org/10.2113/gsecongeo.93.8.1307.
Wellman, P., Dooley, J.C., 1992. Structure of the Mount Isa region inferred from gravity and magnetic anomalies. Explor. Geophys. (Melbourne) 23 (1–2), 417–421. https://doi.org/10.1071/EG992417.
Whittle, M.A., 1998. Aspects of the geology of the Dugald River (zinc-lead) deposit, northwest Queensland, Australia. thesis James Cook University of North Queensland, p. 163 pp.. Unpublished MSc.
Williams, P. (2017). Dugald River Petrography: Summary of Key Observations from the 2017 Knowledge Study. Unpublished report by Clump Mountain Geoscience.
Withnall, I.W., Hutton, L.J. (2013). North Australian Craton, in: Jell, P.A. (Ed.), Geology of Queensland. Geological Survey of Queensland, pp. 23–112.
Wyborn, L., 1998. Younger ca 1500 Ma granites of the Williams and Naraku batholiths, Cloncurry District, eastern Mt Isa Inlier; geochemistry, origin, metallogenic significance and exploration indicators. Aust. J. Earth Sci. 45 (3), 397–411. https://doi.org/10.1080/08120099808728400.
Xu, G., 1996. Structural geology of the Dugald River Zn-Pb-Ag deposit, Mount Isa Inlier, Australia. Ore Geol. Rev. 11 (6), 339–361. https://doi.org/10.1016/S0169-1368(96)00007-8.
Xu, G., 1997. Microstructural evidence for an epigenetic origin of a Proterozoic zinc-lead-silver deposit, Dugald River, Mount Isa Inlier, Australia. Mineralium Deposita 32 (1), 58–69. https://doi.org/10.1007/s001260050072.
Xu, G., 1998a. A fluid inclusion study of syntectonic Zn-Pb-Ag mineralization at Dugald River, Northwest Queensland, Australia. Econ. Geol. 93 (8), 1165–1179. https://doi.org/10.2113/gsecongeo.93.8.1165.
Xu, G., 1998b. Geochemistry of sulphide minerals at Dugald River, NW Queensland, with reference to ore genesis. Mineral. Petrol. 63 (1-2), 119–139. https://doi.org/10.1007/BF01162771.
Zhang, Y., Sun, F., Li, B., Huo, L., Ma, F., 2014. Ore textures and remobilization mechanisms of the Hongtoushan copper-zinc deposit, Liaoning, China. Ore Geol. Rev. 57, 78–86. https://doi.org/10.1016/j.oregeorev.2013.09.006.